

Joint Model Order Selection and Parameter Estimation of Chirps With Harmonic Components

Yaron Doweck, *Student Member, IEEE*, Alon Amar, *Member, IEEE*, and Israel Cohen, *Fellow, IEEE*

Abstract—We consider the problem of jointly determining the number of harmonic components of a fundamental linear chirp, and estimating its parameters (i.e., its initial frequency and frequency rate), given time samples of the observed signal. Common model order criteria select the number of harmonics based on the maximum likelihood estimator. We develop exact and approximated maximum likelihood estimators of these parameters. To avoid an exhaustive search in the initial frequency-frequency rate space involved by those estimators, we propose an alternative low-complexity two-step estimation method. The first step separates the signal to its harmonic components. Then, in the second step, the parameters of interest are estimated using least squares method given the phases of the harmonic components. The method is compared to the exact and approximated maximum likelihood estimators and to the well-known high-order ambiguity function based method. Numerical simulations and real data examples demonstrate that the proposed low-complexity method can successfully replace the maximum likelihood estimator in the model order criteria at moderate to high signal-to-noise ratio. Since the estimates obtained by the proposed method achieve the Cramer-Rao lower bound at these signal to noise ratios.

Index Terms—Cramer-Rao lower bound, harmonic chirps, maximum likelihood estimation.

I. INTRODUCTION

THE problem of estimating the fundamental frequency of harmonic time-stationary sinusoids has wide applications in speech processing, communication, radar and sonar, biomedical systems, electrical power, and semiconductor devices [1]–[11]. The fundamental frequency is assumed to be constant during the observation segment, and this assumption sets a constraint on the possible length of the observation segment. Short segments will ensure that the assumption is valid, but better estimation accuracy is achieved if long segments are used as the signal-to-noise ratio (SNR) is increased.

In some other applications the signal is more appropriately modeled as a sum of harmonic components of a non-stationary

signal, i.e., a signal that its frequency content is varied with respect to (w.r.t.) time, also known as a chirp signal [12]–[14]. For example, in active transmission used in tissue harmonic imaging in ultrasound [15] or by mammals [13], [14] (e.g., bats, dolphins, whales) the signal is deliberately transmitted as a sum of harmonic linear frequency modulated (LFM) chirps to increase the detectability of the source of interest, e.g., an organ in ultrasound or a prey in case of mammals. Such harmonic signals also occur in other applications due to propagation through a non-linear media including rotating machinery in vibrational analysis, music and formants in audio and speech processing, electrical power systems, and target localization [16], [17]. Harmonics of higher orders of frequency modulated chirps, known as polynomial phase signals (PPS) [18]–[20], or non-linear frequency modulated chirps (e.g., hyperbolic frequency modulated signals [13]), are also used in synthetic aperture radar [21], biomedical [22], radio communications, or marine mammals [13], [14].

Estimating the parameters of chirp signals has received much attention in literature and has a wide variety of applications. It is used, for example, in radar [23], vehicle tracking [24], sonar [16], [17], [20] and underwater communication. Methods for estimating the parameters of a mono-component LFM include using maximum likelihood [25], rank reduction techniques [26], [27], ambiguity function [28] and the Wigner-Ville distribution [29]. Methods for estimating the parameters of a multi-component LFM are based on combining a time-frequency transform, such as the Wigner-Ville transform, with an image processing technique (e.g., the Hough transform) [30], Monte-Carlo methods such as importance sampling [31] or Markov chain Monte Carlo [32], using time-frequency representations such as the fractional Fourier transform [33], which is suited to LFM chirps, and the high-order phase function [34].

An LFM signal is a specific case of the PPS family. Estimating the parameters of a PPS can be done, for example, using the well-known high order ambiguity function (HAF) [35] based parameters estimation for mono-component PPS [18], [19] and for multi-component signals [36], [37]. The HAF based estimation is an iterative process. In each iteration, the highest remaining coefficient of the PPS is estimated and then subtracted. Therefore, estimation errors propagate to the lower order coefficients. The product high order ambiguity function (PHAF) method, based on multi-lag HAF, offers improved performance with a minor increase in computational complexity [23]. The HAF based estimation methods, and specifically the PHAF, are very popular as they are simple and relatively low complexity methods. Other methods for estimating the parameters of a mono-component PPS include the phase unwrapping

Manuscript received September 23, 2014; revised December 25, 2014; accepted December 27, 2014. Date of publication January 12, 2015; date of current version March 02, 2015. The associate editor coordinating the review of this manuscript and approving it for publication was Prof. Adel Belouchrani. This work was supported by the Israel Science Foundation (grant no. 1130/11).

Y. Doweck and I. Cohen are with the Department of Electrical Engineering, Technion—Israel Institute of Technology, Technion City, Haifa 32000, Israel (e-mail: yarond@tx.technion.ac.il; icohen@ee.technion.ac.il).

A. Amar is with the Signal Processing Department, Acoustics Research Center, Rafael, Haifa 3102102, Israel (e-mail: alonamar@rafael.co.il).

Color versions of one or more of the figures in this paper are available online at <http://ieeexplore.ieee.org>.

Digital Object Identifier 10.1109/TSP.2015.2391075

[38], [39], multi-linear time-frequency representation [40], iterative methods [41], Wigner-Ville distribution [42], nonlinear least-squares (NLS) [43], high-order phase function [44]–[46] and subspace methods [47]. Solutions for multi-component PPS include the NLS method [48], separation of the signal components [20] and multi-linear methods [49].

It is noteworthy to mention that most parameter estimation algorithms for multi-component signals assume that the number of components, i.e., the model order, is known *a priori*. Otherwise, an order selection rule should be applied. Statistical selection criteria, such as the minimum description length (MDL), Akaike information criterion (AIC) or maximum *a posteriori* probability (MAP) [50], has been successfully applied to multi-components sinusoids [51], [52] and sinusoids with harmonic components [53].

In this work we address the problem of estimating the parameters of the fundamental LFM chirp when the number of harmonic components is unknown. As opposed to multi-component chirps estimation problem, it only considers two parameters of interest, i.e., the initial frequency and frequency rate of the fundamental LFM chirp. Estimation methods of these two parameters for such model have not been presented in literature to date, and thus it is the motivation of the current work.

The model of harmonic components of a fundamental LFM chirp can be considered as a special case of the multi-component chirps estimation problem. Obviously, one can argue that the parameters of each harmonic component can be estimated using any of the multi-component estimation method mentioned above. The parameters of the fundamental LFM can then be determined, e.g., by properly averaging the previous estimates. However, as we later show, this yields a sub-optimal estimation that does not achieve the Cramer-Rao lower bound (CRLB), even in high SNR.

We start by presenting two model order selection criteria, the MDL and AIC. Both of them are based on the maximum likelihood estimator (MLE). We then derive the computationally intensive MLE and suggest a reduced complexity estimator. Both estimators require a two-dimensional high resolution search, in the order of N^4 points to achieve the CRLB, where N is the number of samples. We present two low complexity sub-optimal estimation methods. The first is a modification of the well-known PHAF method for signals with harmonic components. We then propose a new estimation method, harmonic separate-estimate (Harmonic-SEES). It is based on the separate-estimate (SEES) approach, used for estimating the coefficients of a constant modulus signals [20]. The Harmonic-SEES uses the fast Fourier transform (FFT) to obtain a coarse estimation of the parameters and separate the harmonic components. Once separated, the parameters are estimated using a joint least-squares (LS) given the phases of the components.

We show that asymptotically, given a large number of data samples, the Harmonic-SEES estimator is unbiased, and obtain a closed-form expression for its theoretical covariance matrix. We evaluate the computation load of all four estimation methods and show that the MLE involves an order of N^6 and N^5 multiplications per harmonic component for the exact and approximated solutions, respectively, and the Harmonic-SEES only involves an order of $N^2 \log N$ multiplications per harmonic com-

ponent, which is substantially smaller computational load. We show through simulations that the proposed method achieves the CRLB in moderate to high SNR and can be used instead of the MLE in order to estimate the number of harmonic components.

II. PROBLEM STATEMENT AND MODEL ASSUMPTIONS

Consider a discrete-time signal composed of M attenuated harmonic components observed in the presence of noise,

$$x[n] = \sum_{m=1}^M a_m s_m[n] + v[n], \quad n = 0, \dots, N-1 \quad (1)$$

where M is unknown, $a_m = |a_m|e^{j\mu_m}$ is the unknown attenuation of the m th harmonic, $|a_m|$ is the magnitude and μ_m is the phase, and $v[n]$ is a zero mean white circularly symmetric Gaussian discrete-time process representing the additive noise with an unknown variance σ_v^2 . The m th harmonic component in discrete-time is

$$s_m[n] = e^{j\phi_m[n]}, \quad n = 0, \dots, N-1 \quad (2)$$

$$m = 1, \dots, M$$

where the phase is defined as $\phi_m[n] = 2\pi m(\theta_1 n + \frac{1}{2}\theta_2 n^2)$ where $\theta_1 = F_0/F_s$ and $\theta_2 = \beta_0/F_s^2$ are the normalized initial frequency and normalized frequency rate, where F_s is the sampling frequency, F_0 is the initial frequency of the fundamental harmonic, and $\beta_0 = B/T$ is the frequency rate of the fundamental harmonic, where B and T are the signal bandwidth and duration time of the fundamental harmonic, respectively. Also, $N = TF_s$ is the total number of data samples. We assume that the length of the observed signal equals the length of the chirp, which can be obtained by first detecting the presence of the signal and then determining its start and end times. We further assume that $F_s \geq 2 \cdot \max\{MF_0, M(F_0 + \beta_0 T)\}$, where the first and second arguments correspond to the case of decreasing and increasing chirp harmonics, respectively. Finally, note that the differences between the initial (or final) frequencies of the chirps are F_0/F_s (or $(F_0 + \beta_0 T)/F_s$) in case of increasing (or decreasing) chirps. Thus, to ensure that the harmonic components are well separated, we assume that the $\min\{F_0/F_s, (F_0 + \beta_0 T)/F_s\} \geq \delta$, where δ is a pre-defined frequency interval.

By collecting the N samples of the received signal in (1) we obtain a compact vector-form model given as,

$$\mathbf{x} = \mathbf{S}_M \mathbf{a}_M + \mathbf{v} \quad (3)$$

where we define $\mathbf{x} = [x[0], \dots, x[N-1]]^T$, $\mathbf{S}_M = [\mathbf{s}_1, \dots, \mathbf{s}_M]$, $\mathbf{s}_m = [s_m[0], \dots, s_m[N-1]]^T$, $\mathbf{a}_M = [a_1, \dots, a_M]^T$, and $\mathbf{v} = [v[0], \dots, v[N-1]]^T$. The unknown parameter vector of the model is $\boldsymbol{\psi} = [\boldsymbol{\theta}^T, \mathbf{a}_M^T, \sigma_v^2]^T$, where $\boldsymbol{\theta} = [\theta_1, \theta_2]^T$ is the parameter vector of interest. A necessary condition to ensure a unique estimate of $\boldsymbol{\psi}$ requires that the number of measurements, N , is larger than the number of unknowns, $M+2$. i.e., we assume that $N \geq M+2$. The problem herein is: Given the observation vector, \mathbf{x} , estimate the unknown parameter vector, $\boldsymbol{\psi}$, and the model order, M .

III. MODEL ORDER SELECTION

When the number of harmonics is unknown, a model order selection criterion should be used to choose the correct order, M . Two commonly used criteria are the MDL and AIC [50]. Both have the same form, which includes two terms: 1) the minimum of the negative log-likelihood function, $\ell(\hat{\boldsymbol{\psi}} | m)$, where $\hat{\boldsymbol{\psi}}$ is the MLE of $\boldsymbol{\psi}$ and 2) a penalty term, a monotonically increasing function w.r.t the model order designed to prevent over estimation, $p(m)$. That is

$$\begin{aligned} \hat{M} &= \operatorname{argmin}_{m=1,\dots,D} \left\{ \min_{\boldsymbol{\psi}} \ell(\boldsymbol{\psi} | m) + p(m) \right\} \\ &= \operatorname{argmin}_{m=1,\dots,D} \{ \ell(\hat{\boldsymbol{\psi}} | m) + p(m) \} \end{aligned} \quad (4)$$

where D is the highest possible model order.

In the current case, the observation vector in (3) is distributed as a complex multivariate circularly Gaussian random vector, $\mathbf{x} \sim \mathcal{N}_C(\mathbf{S}_m \mathbf{a}_m, \sigma_v^2 \mathbf{I}_N)$, where \mathbf{I}_N is the $N \times N$ identity matrix. The negative log likelihood function of the signal in (3) is obtained by taking the natural logarithm of its probability density function (pdf) conditioned on both the parameter vector, $\boldsymbol{\psi}$, and an assumed model order m . The minimum of the negative log likelihood is given by

$$\ell(\hat{\boldsymbol{\psi}} | m) = \frac{1}{2\sigma_v^2} \|\mathbf{x} - \hat{\mathbf{S}}_m \hat{\mathbf{a}}_m\|^2 + \frac{N}{2} \log(\sigma_v^2) + \log(K) \quad (5)$$

where K is a constant and $(\hat{\cdot})$ denotes the MLE estimate given a number of harmonics. The penalty terms for each criterion are given by [54]

$$p(m) = \begin{cases} \frac{1}{2}(2m+2) \log(N), & \text{MDL} \\ 2m+2, & \text{AIC} \end{cases} \quad (6)$$

where $2m+2$ is the number of unknown parameters. A Bayesian approach can also be used to derive a MAP selection criterion. However, the result, for this case, is equivalent to the MDL criterion [24].

IV. MAXIMUM LIKELIHOOD ESTIMATION

We present an exact MLE for a given number of harmonics, which requires an exhaustive search in the normalized initial frequency-frequency rate space, and involves a large number of computations at each candidate point in this space. It is known that chirps with different time varying frequencies are almost orthogonal. Based on this result and in order to reduce the computations, we further derive the approximated MLE. We term this estimator as the Harmochirp-gram since it extends the idea of the Harmogram [7] used for estimating harmonic sinusoids. This estimator still requires a search in the normalized initial frequency-frequency rate space. However, the cost function obtained requires less computations at each point in this space. Simulation results show that the orthogonality approximation is reasonable as the estimation performances of both estimators are similar.

A. The Exact MLE

As noted above, the MLE of $\boldsymbol{\psi}$ is found by minimizing (5). Assuming some model order, m , the MLE of \mathbf{a}_m , de-

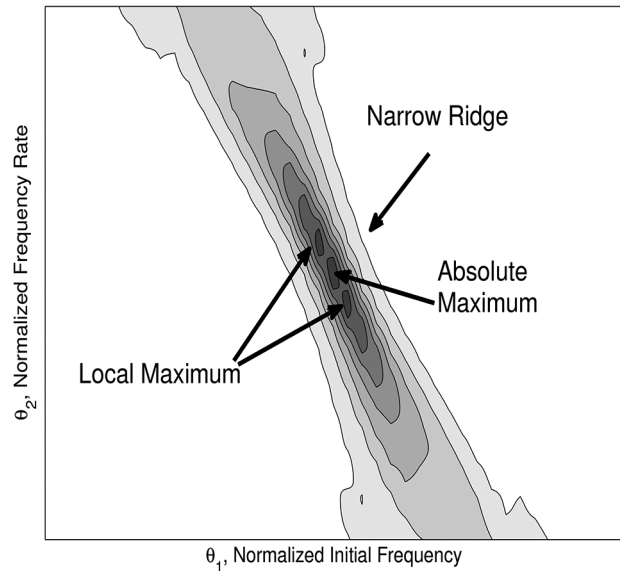


Fig. 1. Illustration of the cost function of the exact MLE.

noted by $\hat{\mathbf{a}}_m$, is obtained by taking the derivative of (5) w.r.t. \mathbf{a}_m^H , and equating the derivative to zero. This results in $\hat{\mathbf{a}}_m = (\mathbf{S}_m^H \mathbf{S}_m)^{-1} \mathbf{S}_m^H \mathbf{x}$. Substituting this estimate in (5) yields the MLE of $\boldsymbol{\theta}$, denoted by $\hat{\boldsymbol{\theta}}_m^{(\text{MLE})}$,

$$\hat{\boldsymbol{\theta}}_m^{(\text{MLE})} = \operatorname{argmax}_{\boldsymbol{\theta}} \{ Q_e(\boldsymbol{\theta}) = \mathbf{x}^H \mathbf{P}_{\mathbf{S}_m} \mathbf{x} \} \quad (7)$$

where $\mathbf{P}_{\mathbf{S}_m} = \mathbf{S}_m (\mathbf{S}_m^H \mathbf{S}_m)^{-1} \mathbf{S}_m^H$ is the projection matrix of \mathbf{S}_m .

In Fig. 1 we present an illustration of the cost function, $Q_e(\boldsymbol{\theta})$, in the (θ_1, θ_2) space. The cost function is composed from a narrow ridge, centered around the location of the true parameters and several local maximums at normalized initial frequency and normalized frequency rates that are half, twice, four times etc. the true fundamental normalized initial frequency and normalized frequency rate, where in high noise scenario, the estimator may yield false estimates.

Unfortunately, there is no closed-form expression for this estimator. Therefore, a two-dimensional exhaustive search in the initial frequency-frequency rate is required. Finally, taking the derivative w.r.t. σ_v^2 and equating to zero yields

$$\hat{\sigma}_{v,m}^2 = \frac{1}{N} \mathbf{x}^H \hat{\mathbf{P}}_{\mathbf{S}_m}^\perp \mathbf{x} \quad (8)$$

where $\hat{\mathbf{P}}_{\mathbf{S}_m}^\perp = \mathbf{I}_N - \hat{\mathbf{P}}_{\mathbf{S}_m}$. Substituting (8) into (5) results in

$$\ell(\hat{\boldsymbol{\psi}} | m) = \frac{N}{2} + \frac{N}{2} \log(\hat{\sigma}_{v,m}^2) + \log(K) \quad (9)$$

Substituting (9) into (4) and discarding all constants yields

$$\hat{M} = \operatorname{argmin}_{m=1,\dots,D} \left\{ \log(\hat{\sigma}_{v,m}^2) + \frac{2}{N} p(m) \right\}. \quad (10)$$

B. The Approximated MLE

The basic assumption of the approximated MLE is that for large number of samples, the cross-product between the ℓ th and k th harmonic components ($\ell \neq k$) is negligible w.r.t. N , i.e.,

$\sum_{n=0}^{N-1} s_\ell^*[n]s_k[n] \ll N$. We thus obtain that, for large number of samples, $\mathbf{S}^H \mathbf{S} \cong N \mathbf{I}_M$. We can then replace the cost function $Q_e(\boldsymbol{\theta})$ in (7) by $Q_a(\boldsymbol{\theta}) = \|\mathbf{S}^H \mathbf{x}\|^2 = \sum_{m=1}^M |s_m^H \mathbf{x}|^2$. We further note that

$$\begin{aligned} Q_a(\boldsymbol{\theta}) &= \sum_{m=1}^M \left| \sum_{n=0}^{N-1} x_m^{(\theta_2)}[n] e^{-j2\pi m \theta_1 n} \right|^2 \\ &= \sum_{m=1}^M \left| \bar{x}_m^{(\theta_2)}(m\theta_1) \right|^2 \end{aligned} \quad (11)$$

where

$$x_m^{(\theta_2)}[n] = x[n] e^{-j2\pi \frac{1}{2} m \theta_2 n^2} \quad (12)$$

and $\bar{x}_m^{(\theta_2)}(m\theta_1) = \sum_{n=0}^{N-1} x_m^{(\theta_2)}[n] e^{-j2\pi \cdot m \theta_1 \cdot n}$ is the discrete time Fourier transform (DTFT) of $x_m^{(\theta_2)}[n]$ computed at the normalized frequency $m\theta_1$. We term the cost function in (11) as the Harmochirp-gram. In addition, (12) is termed the de-chirping of $x[n]$ since it transforms a chirp with frequency rate of $m\theta_2$ into a constant frequency signal.

The estimated parameters using (11) are not the exact MLE for finite data lengths, but are asymptotically efficient when the number of samples is large. To obtain these estimates we actually perform the following steps for each candidate point (θ_1, θ_2) : 1) given θ_2 , we de-chirp the observed signal with a set of normalized frequency rates $\{m\theta_2\}_{m=1}^M$ which yields the signals $\{x_m^{(\theta_2)}[n]\}_{m=1}^M$; 2) Taking the DTFT of each de-chirped signal, $x_m^{(\theta_2)}[n]$, at normalized frequency, $\{m\theta_1\}_{m=1}^M$, and combining the absolute values of the M DTFT at these frequencies (the second step is similar to the Harmogram technique [7] which is used to estimate the fundamental frequency of harmonic sinusoids).

Observe that by substituting (1) into (12) and assuming that θ_2 equals the true normalized frequency rate, $\theta_{2,0}$, we get that

$$x_m^{(\theta_2)}[n] = a_m e^{j2\pi m \theta_{1,0} n} + r_{\theta_{2,0}}[n] + v_{\theta_{2,0}}[n] \quad (13)$$

where $\theta_{1,0}$ is the true normalized initial frequency, $v_{\theta_{2,0}}[n] = v[n] e^{-j2\pi \frac{1}{2} m \theta_{2,0} n^2}$, and $r_{\theta_{2,0}}[n] = \sum_{\substack{k=1 \\ k \neq m}}^M a_k e^{j2\pi \frac{1}{2} (k-m) \theta_{2,0} n^2} e^{j2\pi k \theta_{1,0} n}$ are the de-chirped noise and the residual term due to de-chirping the other harmonic components. That is,

$$\begin{aligned} \bar{x}_m^{(\theta_2)}[n](m\theta_1) \\ \cong a_m D(m(\theta_{1,0} - \theta_1)) + \bar{r}_{\theta_{2,0}}(m\theta_1) + \bar{v}_{\theta_{2,0}}(m\theta_1) \end{aligned} \quad (14)$$

where $D(\theta) = \sum_{n=0}^{N-1} e^{-j2\pi \theta n}$ is the Dirichlet kernel which equals N at $\theta = 0$. Assume that the noise term in (14) is negligible and consider the case where $\theta_1 = \theta_{1,0}$. The first term then equals $a_m N$ while the second term is approximately zero according to the analysis in [55]. Approximately, the value of $Q_a(\boldsymbol{\theta})$ in (11) at the true point is then $Q_a(\theta_{1,0}, \theta_{2,0}) \cong N^2 \sum_{m=1}^M |a_m|^2$ which means that the Harmochirp-gram combines the energies of all the harmonic components together.

In order to understand how large the number of samples is required to be in order for the orthogonality assumption to hold,

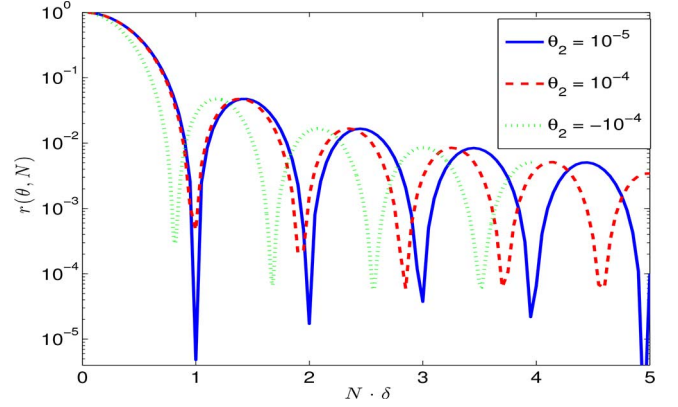


Fig. 2. The ratio between the main and first diagonals of $\mathbf{S}^H \mathbf{S}$.

we wish to examine the ratio between the main and first diagonals of $\mathbf{S}^H \mathbf{S}$

$$r(\boldsymbol{\theta}, N) = \left| \frac{\mathbf{s}_m^H \mathbf{s}_{m+1}}{\mathbf{s}_m^H \mathbf{s}_m} \right|^2 = \left| \frac{1}{N} \sum_{n=0}^{N-1} e^{-j2\pi(\theta_1 n + \frac{1}{2} \theta_2 n^2)} \right|^2. \quad (15)$$

Note that (15) is independent of m and thus holds for each $m = 1, \dots, M$. For $\theta_2 = 0$, we get that $r(\boldsymbol{\theta}, N)$ is the magnitude of the DTFT of a rectangular window with length N . Fig. 2 present $r(\boldsymbol{\theta}, N)$ versus $N \cdot \delta$ for three different values of θ_2 . As it can be seen, θ_2 has a scaling effect on $r(\boldsymbol{\theta}, N)$. Again, considering the case of $\theta_2 = 0$, then $r(\boldsymbol{\theta}, N)$ has a local minimum at $N \cdot \delta = k$, $k = 1, 2, \dots$, a side-lobe level of -13 dB and side-lobes fall rate of -6 dB/octave [56]. Hence, in order to assure more than 20 dB attenuation, we require that

$$N > \frac{3}{\delta}. \quad (16)$$

Note that the scaling, caused by θ_2 , means that (16) ensures that the cross product between two components is sufficiently small for each θ_2 .

C. Computational Load

We evaluate the computational complexity of the Harmochirp-gram and the MLE method by calculating the number of on-line real multiplications involved in each method. Consider first the Harmochirp-gram in (11). Assume that the number of possible values of θ_1 and θ_2 are n_1 and n_2 , respectively. At each point, we perform M times de-chirping and DTFT at a single frequency. The de-chirping and the squared magnitude of the DTFT requires $\mathcal{O}(N)$ multiplications. The total number of real multiplications is $\mathcal{O}(n_1 n_2 M N)$. Note that in order to achieve the CRLB, n_1 and n_2 should be in the order of $N^{3/2}$ and $N^{5/2}$, respectively. Therefore the complexity of the Harmochirp-gram is $\mathcal{O}(N^5 M)$. The exact MLE involves the calculation of (7) at each point. This requires inversion of an $M \times M$ matrix and multiplication of an $N \times M$ matrix by $M \times N$ matrix. Assuming $N \gg M$, the total complexity of the exact MLE is $\mathcal{O}(N^6 M)$.

V. THE CRAMER-RAO LOWER BOUND

The covariance matrix of any unbiased estimate of $\boldsymbol{\psi}$, denoted by $\text{cov}(\hat{\boldsymbol{\psi}}) = E[(\hat{\boldsymbol{\psi}} - \boldsymbol{\psi})(\hat{\boldsymbol{\psi}} - \boldsymbol{\psi})^T]$, is lower bounded by the inverse of the Fisher information matrix (FIM), denoted by $\mathbf{J}_{\boldsymbol{\psi}, \boldsymbol{\psi}}$, that is, $\text{cov}(\hat{\boldsymbol{\psi}}) \geq \mathbf{J}_{\boldsymbol{\psi}, \boldsymbol{\psi}}^{-1}$, where

$$\mathbf{J}_{\boldsymbol{\psi}, \boldsymbol{\psi}} = \begin{bmatrix} \mathbf{J}_{\boldsymbol{\theta}, \boldsymbol{\theta}} & \mathbf{J}_{\boldsymbol{\theta}, \mathbf{a}} & \mathbf{0} \\ \mathbf{J}_{\boldsymbol{\theta}, \mathbf{a}}^T & \mathbf{J}_{\mathbf{a}, \mathbf{a}} & \mathbf{0} \\ \mathbf{0}^T & \mathbf{0}^T & \mathbf{J}_{\sigma_v^2, \sigma_v^2} \end{bmatrix} \quad (17)$$

where the sub-matrices of $\mathbf{J}_{\boldsymbol{\psi}, \boldsymbol{\psi}}$ are shown to be given by (see the Appendix)

$$\mathbf{J}_{\boldsymbol{\theta}, \boldsymbol{\theta}} = \frac{4\pi^2}{\sigma_v^2} \begin{bmatrix} 2\mathbf{W}_1 & \mathbf{W}_2 \\ \mathbf{W}_2 & \mathbf{W}_3 \end{bmatrix} \quad (18)$$

$$\mathbf{J}_{\mathbf{a}, \mathbf{a}} = \frac{2}{\sigma_v^2} \begin{bmatrix} (\mathbf{S}^H \mathbf{S})_r & (\mathbf{S}^H \mathbf{S})_i \\ -(\mathbf{S}^H \mathbf{S})_i & (\mathbf{S}^H \mathbf{S})_r \end{bmatrix} \quad (19)$$

$$\mathbf{J}_{\boldsymbol{\theta}, \mathbf{a}} = \frac{2\pi}{\sigma_v^2} \begin{bmatrix} 2(\mathbf{U}_1)_i & 2(\mathbf{U}_1)_r \\ (\mathbf{U}_2)_i & (\mathbf{U}_2)_r \end{bmatrix} \quad (20)$$

where $\mathbf{x}_r = \Re\{\mathbf{x}\}$ and $\mathbf{x}_i = \Im\{\mathbf{x}\}$ denote the real and imaginary parts of \mathbf{x} , respectively. Also, $\mathbf{W}_i = \|\mathbf{Q}^{(i+1)/2} \mathbf{S} \mathbf{D} \mathbf{a}\|^2$, $i = 1, 2, 3$, $\mathbf{U}_i = \mathbf{a}^H \mathbf{D}^T \mathbf{S}^H \mathbf{Q}^i \mathbf{S}$, $i = 1, 2$ with $\mathbf{D} = \text{diag}(1, 2, \dots, M)$ and $\mathbf{Q} = \text{diag}(0, 1, \dots, N-1)$, where we defined $\mathbf{A}^k = \text{diag}(a_1^k, \dots, a_L^k)$ for real k . Using the matrix inversion lemma ([55], App. A) we get that the CRLB on $\boldsymbol{\theta}$ is then given by

$$\text{cov}(\hat{\boldsymbol{\theta}}) \geq (\mathbf{J}_{\boldsymbol{\theta}, \boldsymbol{\theta}} - \mathbf{J}_{\boldsymbol{\theta}, \mathbf{a}} \mathbf{J}_{\mathbf{a}, \mathbf{a}}^{-1} \mathbf{J}_{\boldsymbol{\theta}, \mathbf{a}}^T)^{-1} \quad (21)$$

where $\text{cov}(\hat{\boldsymbol{\theta}}) = E[(\hat{\boldsymbol{\theta}} - \boldsymbol{\theta})(\hat{\boldsymbol{\theta}} - \boldsymbol{\theta})^T]$ is the covariance of $\hat{\boldsymbol{\theta}}$.

A. The Large-Samples Approximation of the CRLB

Observe that the terms $\{\mathbf{S}^H \mathbf{Q}^u \mathbf{S}\}_{u=0}^4$ appears in the expressions of $\mathbf{J}_{\boldsymbol{\theta}, \boldsymbol{\theta}}$ and $\mathbf{J}_{\boldsymbol{\theta}, \mathbf{a}}$ via the matrices $\{\mathbf{W}_i\}_{i=1}^3$, and $\{\mathbf{U}_i\}_{i=1}^2$. The (ℓ, k) th element of $\{\mathbf{S}^H \mathbf{Q}^u \mathbf{S}\}_{u=0}^4$ is given by,

$$\mathbf{s}_\ell^H \mathbf{Q}^u \mathbf{s}_k = \sum_{n=0}^{N-1} n^u e^{-j2\pi(\ell-k)\frac{1}{2}\theta_{2,0}n^2} e^{-j2\pi(\ell-k)\theta_{1,0}n} \quad (22)$$

The value of $\mathbf{S}^H \mathbf{Q}^u \mathbf{S}$ along the main diagonal is $\sum_{n=0}^{N-1} n^u$, which for $N \gg 1$, is approximately $N^{u+1}/(u+1)$. We assume that for $N \gg 1$, $\mathbf{S}^H \mathbf{Q}^u \mathbf{S} \cong \frac{N^{u+1}}{u+1} \mathbf{I}_M$, i.e., we neglect the off-diagonal terms of the matrix. We thus obtain after few simple mathematical steps that the different FIM in (18)–(20) are approximately given as

$$\mathbf{J}_{\boldsymbol{\theta}, \boldsymbol{\theta}} \cong \frac{\pi^2 N^3}{\sigma_v^2} \begin{bmatrix} \frac{8}{3} \mathbf{a}^H \mathbf{D}^2 \mathbf{a} & N \mathbf{a}^H \mathbf{D}^2 \mathbf{a} \\ N \mathbf{a}^H \mathbf{D}^2 \mathbf{a} & \frac{2N^2}{5} \mathbf{a}^H \mathbf{D}^2 \mathbf{a} \end{bmatrix} \quad (23)$$

$$\mathbf{J}_{\mathbf{a}, \mathbf{a}} \cong \frac{2N}{\sigma_v^2} \mathbf{I}_M \quad (24)$$

$$\mathbf{J}_{\boldsymbol{\theta}, \mathbf{a}} \cong \frac{2\pi N^2}{\sigma_v^2} \begin{bmatrix} -\mathbf{a}_i^T \mathbf{D} & \mathbf{a}_r^T \mathbf{D} \\ -\frac{N}{3} \mathbf{a}_i^T \mathbf{D} & \frac{N}{3} \mathbf{a}_r^T \mathbf{D} \end{bmatrix} \quad (25)$$

Substituting (23)–(25) in (21) yields that the large-samples CRLB on the parameter vector $\boldsymbol{\theta}$ is given by,

$$\text{cov}(\hat{\boldsymbol{\theta}}) \geq \frac{1}{\mathbf{a}_M^H \mathbf{D}^2 \mathbf{a}_M} \frac{\sigma_v^2}{\pi^2 N^3} \begin{bmatrix} 24 & -\frac{45}{N} \\ -\frac{45}{N} & \frac{90}{N^2} \end{bmatrix}. \quad (26)$$

The large-samples CRLB on the estimation error of the normalized initial frequency and frequency rate are,

$$E[\theta_1^2] \geq \frac{24\sigma_v^2}{\pi^2 N^3} \frac{1}{\mathbf{a}^H \mathbf{D}^2 \mathbf{a}}, \quad E[\theta_2^2] \geq \frac{90\sigma_v^2}{\pi^2 N^5} \frac{1}{\mathbf{a}^H \mathbf{D}^2 \mathbf{a}}. \quad (27)$$

Observe that $\mathbf{a}^H \mathbf{D}^2 \mathbf{a} = \sum_{m=1}^M m^2 |a_m|^2 < \sum_{m=1}^M m^2 = (M+1)M(2M+1)/6$, where the inequality holds for $|a_m| \leq 1$. By estimating the normalized initial frequency and frequency rate using all the M harmonic components, we improve the estimation error w.r.t. M^3 . Furthermore, the estimation accuracy of θ_1 and θ_2 decrease as $1/N^{3/2}$ and $1/N^{5/2}$, respectively, which can be obtained using the DTFT as is being used by the Harmonic-gram.

VI. PRODUCT HIGH ORDER AMBIGUITY FUNCTION

The PHAF method for estimating parameters of a multi component PPS was introduced in [23]. It is a low complexity sub-optimal estimation method that uses multi-lag HAF [18] to reduce the dimension of the problem to one dimensional search. We now wish to present the methods and its application to the estimation of the parameters of harmonic LFM signals.

The second order ambiguity function is defined as [23]

$$X_2(\theta; \tau) = \sum_{n=0}^{N-1} x_2[n; \tau] e^{-j2\pi\omega n} \quad (28)$$

where $x_2[n; \tau] = x[n]x^*[n - \tau]$ and τ is a delay, in samples. The ambiguity function, when applied to LFM, transform the signal into a complex sinusoids [23]. That is, $x_2[n; \tau]$ will be a sum of M complex sinusoids at the frequencies $\theta_m = \tau m \theta_2$. Therefore, $X_2(\theta; \tau)$ should have M strong peaks at the expected frequencies. Given a set of L lags, $\boldsymbol{\tau} = [\tau_1, \dots, \tau_L]$, the PHAF is defined as a product of L scaled second order ambiguity functions

$$X_2(\theta; \boldsymbol{\tau}) = \prod_{\ell=1}^L X_2(\theta \tau_\ell / \tau_1; \tau_\ell). \quad (29)$$

The scaling procedure aligns the sinusoids to the same frequency. Hence, $X_2(\theta; \boldsymbol{\tau})$ will have very strong peaks at $\theta = \tau_1 \theta_2, \dots, \tau_1 M \theta_2$. Note that (28) is constructed using a DTFT. Thus, a high resolution search is still required. However, as opposed to the MLE, the problem is now reduced to a one dimensional search. As we showed, the required resolution in order to achieve the CRLB is $1/N^{5/2}$.

Following the estimation procedure for a multi-component signals from [23], the parameters are estimated as follows. First, the frequency rates of each component, $\hat{\theta}_2^{(1)}, \dots, \hat{\theta}_2^{(M)}$, are estimated separately by picking the M highest peaks in (29). Then, M de-chirped signals are defined as

$$x_m[n] = x[n] e^{-j2\pi \frac{1}{2} \hat{\theta}_2^{(m)} n^2}. \quad (30)$$

Each de-chirped signal should be composed of a complex sinusoid in presence of interfering harmonics. The initial frequency of each component, $\hat{\theta}_1^{(1)}, \dots, \hat{\theta}_1^{(M)}$, are thus estimated as

$$\hat{\theta}_1^{(m)} = \arg \max_{\theta_1} x_m[n] e^{-j2\pi \theta_1 n}. \quad (31)$$

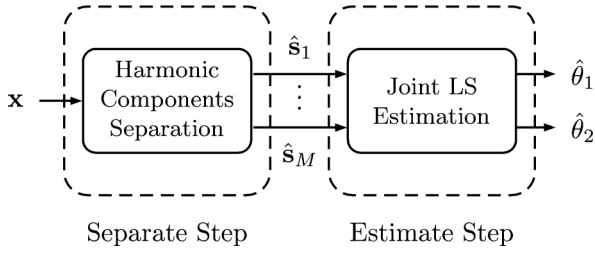


Fig. 3. The Harmonic-SEES estimator.

We define the estimated parameters vectors $\hat{\theta}^{(m)} = [\hat{\theta}_1^{(m)}, \hat{\theta}_2^{(m)}]^T$, $m = 1, \dots, M$. We define a mapping of the components numbers, $f: [1, M] \rightarrow [1, M]$, such that $\hat{\theta}_1^{(f(1))} < \hat{\theta}_1^{(f(2))} < \dots < \hat{\theta}_1^{(f(M))}$. Then, the parameters can be estimated by solving the following LS problem

$$\hat{\theta}^{(\text{PHAF})} = \arg \min_{\theta} \|\mathbf{A}_M \theta - \theta_M\|^2 \quad (32)$$

where

$$\mathbf{A}_M = \begin{bmatrix} \mathbf{g}_M & \mathbf{0}_M \\ \mathbf{0}_M & \mathbf{g}_M \end{bmatrix}, \quad (33)$$

$\mathbf{0}_n$ is the $n \times 1$ vector with all elements equal to zero, $\mathbf{g}_M = [1, \dots, M]^T$ and $\theta_M = [\hat{\theta}_1^{(f(1))}, \dots, \hat{\theta}_1^{(f(M))}, \hat{\theta}_2^{(f(1))}, \dots, \hat{\theta}_2^{(f(M))}]^T$. Solving the above problem yields

$$\hat{\theta}^{(\text{PHAF})} = (\mathbf{A}_M^T \mathbf{A}_M)^{-1} \mathbf{A}_M^T \theta_M = \frac{1}{C_M} \sum_{m=1}^M m \hat{\theta}^{(f(m))} \quad (34)$$

where $C_M = \sum_{m=1}^M m^2 = \frac{1}{6}(M+1)M(2M+1)$.

Once θ is estimated, $\hat{\theta}^{(\text{PHAF})}$ can be substituted in (8) instead of the $\hat{\theta}^{(\text{MLE})}$ in order to estimate the conditional negative log-likelihood and select the number of harmonics according to (10).

A major problem with the PHAF based estimation is that the parameters are estimated separately. Therefore, the estimation error of the frequency rate will propagate to the estimation of the initial frequency [23].

A. Accuracy Analysis

For a single LFM component at high SNR, the PHAF method is known to achieve the CRLB [23]. That is, we assume that the estimated parameters of each component, $\hat{\theta}^{(f(m))}$, is given by $\hat{\theta}^{(f(m))} = m\theta + \epsilon^{(m)}$ where $\epsilon^{(m)}$ is a zero-mean Gaussian process with a covariance given by the CRLB for a single LFM. Therefore, according to (26), we assume that

$$\text{cov}(\epsilon^{(m)}) = \frac{1}{|a_m|^2} \frac{\sigma_{v,m}^2}{\pi^2 N^3} \begin{bmatrix} 24 & -\frac{45}{N} \\ -\frac{45}{N} & \frac{90}{N^2} \end{bmatrix} \quad (35)$$

where $\sigma_{v,m}^2$ accounts for the additive noise and the interference of the other components. We further assume that the errors of any two components are uncorrelated, i.e., $E[(\epsilon^{(m)})^H \epsilon^{(k)}] = 0$ for $m \neq k$. The estimations of each component actually are correlated but we model that as an interference that contribute more

noise. As noted in [23], analyzing $\sigma_{v,m}^2$ is very complicated. We can therefore conclude that

$$\text{var}(\hat{\theta}_1) = \frac{24}{C_M \pi^2 N^3} \sum_{m=1}^M \frac{m \sigma_{v,m}^2}{|a_m|^2} \quad (36)$$

$$\text{var}(\hat{\theta}_2) = \frac{90}{C_M \pi^2 N^5} \sum_{m=1}^M \frac{m \sigma_{v,m}^2}{|a_m|^2} \quad (37)$$

In order to compare the PHAF estimator to the optimal estimator, we examine the ratio between the variance of the MLE and that of the PHAF method

$$\begin{aligned} \frac{\text{var}(\hat{\theta}_k^{(\text{PHAF})})}{\text{var}(\hat{\theta}_k^{(\text{MLE})})} &= \frac{\sum_{m=1}^M m \sigma_{v,m}^2 / |a_m|^2}{C_M} \frac{\sum_{m=1}^M m^2 |a_m|^2}{\sigma_v^2} \\ &> \frac{\sum_{m=1}^M m \sigma_v^2 / |a_m|^2}{C_M} \frac{\sum_{m=1}^M m^2 |a_m|^2}{\sigma_v^2} \\ &= \frac{\sum_{m=1}^M m / |a_m|^2}{C_M} \sum_{m=1}^M m^2 |a_m|^2 \quad (38) \\ &= \frac{1}{C_M} \left(\sum_{m=1}^M m^3 + \sum_{m \neq p} m p^2 |a_p / a_m|^2 \right) \\ &> \frac{\sum_{m=1}^M m^3}{\sum_{m=1}^M m^2} = \frac{3M}{2} \frac{M+1}{2M+1} \\ &> \frac{3M}{2} \frac{M+1}{2M+2} = \frac{3M}{4} \quad (39) \end{aligned}$$

for $k = 1, 2$. The MLE is asymptotically efficient. Therefore, from the last result, we get that for $M \geq 2$ the PHAF estimator cannot, even in high SNR, achieve the CRLB. As shown before, the MLE error improves by a factor of M^3 . From the last result it seems that the PHAF estimator improves only by a factor of M^2 . Generally, since $\sigma_{v,m}^2 > \sigma_v^2$, this is not a tight lower bound and the actual error should be even higher.

B. Computational Load

The construction of the PHAF in (29) involves calculation of a DTFT L times, each requires $\mathcal{O}(N)$ multiplications per frequency. The number of frequency rate candidates required to achieve the best possible approximation is in the order of $N^{5/2}$. The total number of multiplications required to construct (29) is therefore $\mathcal{O}(N^{7/2}L)$. Next, M DTFTs, one for each de-chirped signals are required. The number of frequencies in this step is in the order of $N^{3/2}$. The complexity of the initial frequencies estimation is therefore $\mathcal{O}(MN^{5/2})$. The last step, the LS, requires $\mathcal{O}(M)$ multiplications which is negligible. To conclude, the PHAF method involves $\mathcal{O}(N^{7/2}L)$ multiplications. Since L should be a small number, this is substantially less than the complexity of the Harmochirp-gram estimator.

VII. THE HARMONIC SEPARATE-ESTIMATE METHOD

The use of the DTFT, as demonstrated in the numerical results, makes it possible to achieve the CRLB. However, it re-

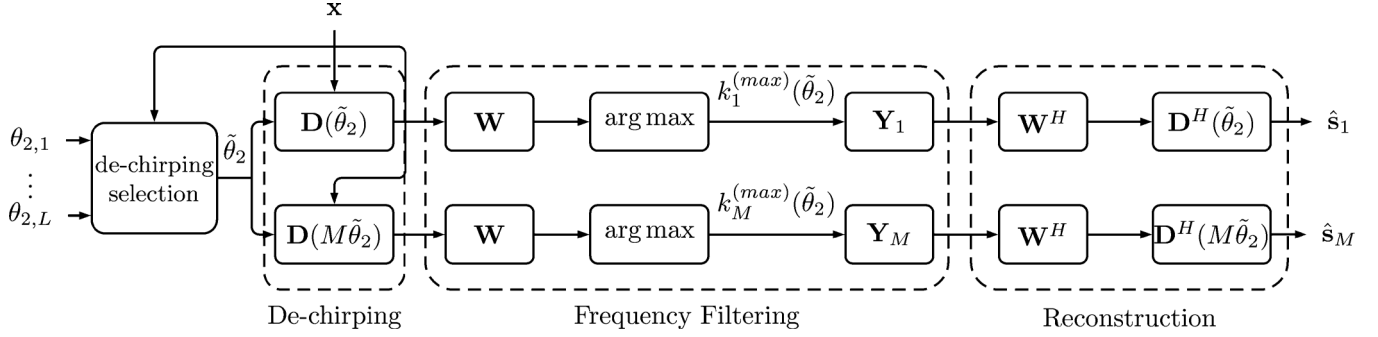


Fig. 4. Scheme of the separate step.

quires large number of computations. This complexity can be reduced using the discrete Fourier transform (DFT) which is more attractive due to its efficient implementation, the FFT. However, the frequency resolution of the DFT is limited proportionally to the inverse of the number of samples, i.e., $1/N$. To overcome this resolution limit but still exploits the low complexity of the DFT, we suggest a suboptimal estimator, the Harmonic-SEES.

We suggest a two-step method to estimate θ_1 and θ_2 of the harmonic chirps (see Fig. 3). First, separate the signal to its harmonic components and then jointly estimate the θ_1 and θ_2 from the phases of the signals using a LS approach. The computationally efficient DFT is used in a separate step to obtain a coarse normalized frequency rate estimate, and this estimate is further refined within the second step using the LS principle. We show that asymptotically, that is, given large number of data samples, the Harmonic-SEES estimator is unbiased, and obtain a closed-form expression for its theoretical covariance matrix.

The outputs of the separate step are M reconstructed harmonic components of the original signal. We design M processors where each processor is composed of three blocks (See Fig. 4): 1) de-chirping; 2) frequency filtering; 3) reconstruction. The first block eliminates the quadratic term of the phase of the m th harmonic component and retains the linear term of the phase only. The second block transforms the de-chirped signal to the frequency domain using DFT, and removes interferences from other harmonic components using a filter which is tuned to the frequency of the m th complex exponential. In the third block the de-chirped and filtered signal is back transformed to the time domain using inverse DFT (IDFT), and is multiplied by a chirp with a normalized frequency rate equals to the de-chirping frequency rate used in the first block of the m th processor. This processing chain assumes that the de-chirping value is given. Hence, we first perform a pre-processing step where we select the suitable de-chirping value. We next describe the separate step in details.

1) *De-Chirping Selection*: We define a set of L de-chirping normalized frequency rates ($L \gg M$) denoted by $\Omega = \{\theta_{2,1}, \dots, \theta_{2,L}\}$. For each $\theta_{2,\ell} \in \Omega$, we define a corresponding harmonic de-chirping set, denoted by $\Omega_\ell = \{\theta_{2,\ell}, 2\theta_{2,\ell}, \dots, M\theta_{2,\ell}\}$ and define the m th de-chirped signal, denoted by $\mathbf{x}_{\ell,m} = [x_{\ell,m}[0], \dots, x_{\ell,m}[N-1]]^T$, where $m = 1, \dots, M$ as

$$\mathbf{x}_{\ell,m} = \mathbf{D}(m\theta_{2,\ell})\mathbf{x} \quad (40)$$

$$\mathbf{D}(m\theta_{2,\ell}) = \text{diag}\left(1, \dots, e^{-j2\pi\frac{1}{2}m\theta_{2,\ell}(N-1)^2}\right) \quad (41)$$

If $\theta_{2,\ell}$ equals the true normalized frequency rate, we get an attenuated complex exponential in the presence of other interfering harmonic components and noise. We thus compute the DFT $x_{\ell,m}[n]$ at the k th frequency bin as $\bar{x}_{\ell,m}[k] = \sum_{n=0}^{N-1} x_{\ell,m}[n]e^{-j\frac{2\pi}{N}kn}$, $k = 0, \dots, N-1$. By defining the DFT vector $\bar{\mathbf{x}}_{\ell,m} = [\bar{x}_{\ell,m}[0], \dots, \bar{x}_{\ell,m}[N-1]]^T$ we obtain,

$$\bar{\mathbf{x}}_{\ell,m} = \mathbf{W}\mathbf{x}_{\ell,m} \stackrel{\text{by (40)}}{=} \mathbf{W}\mathbf{D}(m\theta_{2,\ell})\mathbf{x} \quad (42)$$

where \mathbf{W} is the $N \times N$ DFT transformation matrix. If the de-chirping set $\Omega_\ell = \{\theta_{2,\ell}, 2\theta_{2,\ell}, \dots, M\theta_{2,\ell}\}$ equals to the true set of normalized frequency rates of the M harmonic components, given by $\{\theta_{2,0}, 2\theta_{2,0}, \dots, M\theta_{2,0}\}$, then $\bar{\mathbf{x}}_{\ell,m}$ is the sampled Dirichlet function where the value of the peak of $\bar{\mathbf{x}}_{\ell,m}$, is $N|a_m|$ (neglecting the noise). By summing the values of all peaks together, we obtain a value equals to $N^2 \sum_{m=1}^M |a_m|^2$, which is the energy of the harmonic signal. Any other hypothesized normalized frequency rate will result in a smaller value. Hence, we need to define a criterion for selecting the suitable de-chirping value. One possibility is to select the normalized frequency as,

$$\tilde{\theta}_2 = \underset{\theta_{2,\ell} \in \Omega}{\text{argmax}} \sum_{m=1}^M \left| \bar{x}_{\ell,m} \left[k_m^{(\text{max})}(\theta_{2,\ell}) \right] \right| \quad (43)$$

where $\bar{x}_{\ell,m}[k_m^{(\text{max})}(\theta_{2,\ell})]$ is the maximum value of $\bar{\mathbf{x}}_{\ell,m}[k]$, and the location of the maximum is,

$$k_m^{(\text{max})}(\tilde{\theta}_2) = \underset{k}{\text{argmax}} |\bar{x}_{\ell,m}[k]|. \quad (44)$$

Another possibility is to use a Harmogram-like criterion that will exploit the relationship between the expected $\{k_m^{(\text{max})}(\tilde{\theta}_2)\}$. The normalized frequency is selected as

$$\tilde{\theta}_2 = \underset{\theta_{2,\ell} \in \Omega}{\text{argmax}} \max_k \sum_{m=1}^M |\bar{x}_{\ell,m}[mk]|. \quad (45)$$

Other possible selection criteria can be based on computing the sparsity of $\bar{\mathbf{x}}_{\ell,m}$, e.g., its Kurtosis [57].

2) *Separating the Harmonic Components*: Given $\tilde{\theta}_2$, We filter $\bar{\mathbf{x}}_{\ell,m}$ in the frequency domain with a bandpass filter of length δ (a pre-defined frequency interval that ensures the

harmonic components are well separated) expressed by the matrix,

$$\mathbf{Y}_m = \text{diag} \left(\left[\mathbf{0}_{k_m^{(\max)}(\tilde{\theta}_2) - \delta/2}^T, \mathbf{1}_\delta^T, \mathbf{0}_{N - k_m^{(\max)}(\tilde{\theta}_2) - \delta/2}^T \right]^T \right) \quad (46)$$

where $\mathbf{1}_n$ is the $n \times 1$ vector with all elements equal to one.

As mentioned above, when $\tilde{\theta}_2 = \theta_2$, then $\mathbf{x}_{\ell,m}$ is a complex exponential whose DFT, $\bar{\mathbf{x}}_{\ell,m}$, is a Dirichlet function. However, this is not the case in general. The m th component in $\mathbf{x}_{\ell,m}$ should be an LFM with a very small bandwidth. Assume that the search grid $\{\theta_{2,\ell}\}_{\ell=1}^L$ is uniformly spaced such that $d = \theta_{2,\ell+1} - \theta_{2,\ell}$. Then the bandwidth of the LFM should be no more than Nd . Therefore, in order to avoid filtering the desired signal, the length of the filter should satisfy $\delta \geq Nd$. However, increasing the filter length introduces more noise into the filtered signal which can cause poor estimation.

The filtered signal in the frequency domain is,

$$\bar{\mathbf{s}}_m = \mathbf{Y}_m \bar{\mathbf{x}}_{\ell,m} \stackrel{\text{by (42)}}{=} \mathbf{Y}_m \mathbf{W} \mathbf{D}_m(m\tilde{\theta}_2) \mathbf{x}. \quad (47)$$

Ideally, this process retains an attenuated complex exponential with a frequency equals to the normalized initial frequency of the m th harmonic component. To obtain the original harmonic component of the chirp, we perform an IDFT followed by a chirp multiplication, i.e.,

$$\hat{\mathbf{s}}_m = \mathbf{D}(m\tilde{\theta}_2)^H \mathbf{W}^H \bar{\mathbf{s}}_m \stackrel{\text{by (47)}}{=} \mathbf{G}_m \mathbf{x} \quad (48)$$

where by substituting (47) into (48) we define

$$\mathbf{G}_m = \mathbf{D}(m\tilde{\theta}_2)^H \mathbf{W}^H \mathbf{Y}_m \mathbf{W} \mathbf{D}(m\tilde{\theta}_2). \quad (49)$$

We thus obtain a set of M reconstructed harmonic components, $\{\hat{\mathbf{s}}_1, \dots, \hat{\mathbf{s}}_M\}$, of the observed signal.

Assume that $\{\hat{\mathbf{s}}_m\}_{m=1}^M$ are filtered without interference from other harmonic components. We therefore get that,

$$\hat{\mathbf{s}}_m[n] = |a_m| e^{j\mu_m} s_m[n] + e_m[n] = |\hat{s}_m(n)| e^{j\hat{\phi}_m[n]} \quad (50)$$

where $|\hat{s}_m(n)|$ and $\hat{\phi}_m[n]$ are the absolute value and phase of $\hat{\mathbf{s}}_m[n]$, respectively, $e_m[n]$ is the n th element of $\mathbf{e}_m = \mathbf{G}_m \mathbf{v}$. Assuming that small errors are present, i.e., $|e_m[n]| \ll |a_m|$, $m = 1, \dots, M$, it can be shown using a first order Taylor series that the magnitude and phase in (50) are approximately,

$$\begin{aligned} |\hat{\mathbf{s}}_m[n]| &= |a_m| \cos(\phi_m[n] + \mu_m) + \Re\{e_m[n]\} \\ &\quad + j(|a_m| \sin(\phi_m[n] + \mu_m) + \Im\{e_m[n]\}) \\ &\cong |a_m| + \Re\{e_m[n] e^{-j\mu_m} e^{-j\phi_m[n]}\} \end{aligned} \quad (51)$$

$$\begin{aligned} \hat{\phi}_m[n] &= \tan^{-1} \left(\frac{\sin(\phi_m[n] + \mu_m) + \Im\{e_m[n]\}}{\cos(\phi_m[n] + \mu_m) + \Re\{e_m[n]\}} \right) \\ &\cong \phi_m[n] + \mu_m - \sin(\phi_m[n] + \mu_m) \Re\{e_m[n]\} \\ &\quad + \cos(\phi_m[n] + \mu_m) \Im\{e_m[n]\} \\ &\cong \phi_m[n] + \mu_m + \Im\{e_m[n] e^{-j\mu_m} e^{-j\phi_m[n]}\} \end{aligned} \quad (52)$$

We assume the magnitude of the filtered signal $\hat{\mathbf{s}}_m[n]$ is approximately $|a_m|$. The information on the normalized initial frequency and frequency rate is hidden in the wrapped phases $\{\hat{\phi}_m[n]\}_{n=0, m=1}^{N-1, M}$. However, to estimate the normalized initial frequency and frequency rate, we need to consider the unwrapped phase.

A. Phase Unwrapping

First, we present parameters estimation given the unwrapped phases of $\{\hat{\phi}_m[n]\}_{n=0}^{N-1}$, denoted by $\{\tilde{\phi}_m[n]\}_{n=0}^{N-1}$. In case of LFM signals, the unwrapped phase can be found by integrating the second derivative of the phase of the signal [38] given by

$$\begin{aligned} \Delta^2 \tilde{\phi}_m[n] &= \hat{\phi}_m[n] - 2\hat{\phi}_m[n-1] + \hat{\phi}_m[n-2] \\ &= \arg(\hat{\mathbf{s}}_m[n] (\hat{\mathbf{s}}_m^*[n-1])^2 \hat{\mathbf{s}}_m[n-2]) \end{aligned} \quad (53)$$

for $n = 2, \dots, N$. The motivation is that the second derivative of the phase of an LFM is constant and as such, can be extracted from the signal. By integrating $\Delta^2 \tilde{\phi}_m[n]$ we obtain

$$\Delta \tilde{\phi}_m[n] = \Delta^2 \tilde{\phi}_m[n] + \Delta \tilde{\phi}_m[n-1] \quad (54)$$

where we define $\Delta \tilde{\phi}_m[1] = \arg(\hat{\mathbf{s}}_m[0] \hat{\mathbf{s}}_m^*[1])$. And the unwrapped phase is given by

$$\begin{aligned} \tilde{\phi}_m[0] &= \arg(\hat{\mathbf{s}}_m[0]) \\ &= \hat{\phi}_m(0) \pmod{2\pi} \end{aligned} \quad (55)$$

$$\tilde{\phi}_m[n] = \Delta \tilde{\phi}_m[n] + \tilde{\phi}_m[n-1], \quad n = 1, \dots, N. \quad (56)$$

We further assume that the noises are small enough such that they do not cause any π jumps in the unwrapping procedure. The unwrapped phase at the end of this step is

$$\tilde{\phi}_m[n] = \hat{\phi}_m[n] \cong \mu_m + 2\pi m \left(\theta_1 n + \frac{1}{2} \theta_2 n^2 \right) + \varepsilon_m[n] \quad (57)$$

where we define the error term $\varepsilon_m[n] = \Im\{e_m[n] e^{-j\mu_m} e^{-j\phi_m[n]}\}$. Define the vector of phase measurements obtained from the m th reconstructed harmonic component, $\hat{\mathbf{s}}_m$, by $\tilde{\boldsymbol{\phi}}_m \triangleq [\tilde{\phi}_m[0], \dots, \tilde{\phi}_m[N-1]]^T$. Collecting all the measurements in (57) we obtain an approximate linear model for θ_1 and θ_2 given $\tilde{\boldsymbol{\phi}}_m[n]$, i.e.,

$$\tilde{\boldsymbol{\phi}}_m = \mu_m \mathbf{1}_N + 2\pi m \mathbf{H} \boldsymbol{\theta} + \boldsymbol{\varepsilon}_m, \quad m = 1, \dots, M \quad (58)$$

where $\mathbf{H} = [\mathbf{h}_1, \mathbf{h}_2]$ with $\mathbf{h}_1 = [0, 1, \dots, N-1]^T$, and $\mathbf{h}_2 = [0^2/2, 1^2/2, \dots, (N-1)^2/2]^T$.

Also, $\boldsymbol{\varepsilon}_m = [\varepsilon_m[0], \dots, \varepsilon_m[N-1]]^T = \Im\{e^{-j\mu_m} \mathbf{s}_m^* \odot \mathbf{e}_m\}$ where \odot is the Hadamard (dot) product. The unknown parameters $\{\mu_m\}_{m=1}^M$ and the unknown vector $\boldsymbol{\theta}$ are estimated using a LS method as follows,

$$\begin{aligned} & \left[\{\hat{\mu}_m\}_{m=1}^M, \hat{\boldsymbol{\theta}}^T \right]^T \\ &= \underset{\{\mu_m\}_{m=1}^M, \boldsymbol{\theta}}{\text{argmin}} \sum_{m=1}^M \|\tilde{\boldsymbol{\phi}}_m - \mu_m \mathbf{1}_N - 2\pi m \mathbf{H} \boldsymbol{\theta}\|^2 \end{aligned} \quad (59)$$

Taking the derivative of (59) w.r.t. μ_m and equating the result to zero yields that $\hat{\mu}_m = (\mathbf{1}_N^T \mathbf{1}_N)^{-1} \mathbf{1}_N^T (\hat{\phi}_m - 2\pi m \mathbf{H} \hat{\theta})$. Substituting $\hat{\mu}_m$ into (59), taking the derivative w.r.t. θ and equating the result to zero yields that the estimate of θ is,

$$\hat{\theta} = (\mathbf{H}^T \mathbf{P}_1^\perp \mathbf{H})^{-1} \mathbf{H}^T \mathbf{P}_1^\perp \boldsymbol{\varphi} \quad (60)$$

where $\mathbf{P}_1^\perp = \mathbf{I}_N - \mathbf{1}_N (\mathbf{1}_N^T \mathbf{1}_N)^{-1} \mathbf{1}_N^T$, $\boldsymbol{\varphi} = [\varphi[0], \dots, \varphi[N-1]]^T = \frac{1}{2\pi C_M} \sum_{m=1}^M m \hat{\phi}_m$.

B. Joint Phase Unwrapping and Least Squares

The phase unwrapping process as described above assumes that the unwrapped phase does not change by more than π between two consecutive samples. That is, we assume that $|\Delta \hat{\phi}_m[n]| < \pi$. If $|\Delta \hat{\phi}_m[n]|$ is close to π , the processes becomes very sensitive to noise [39].

To overcome that problem, a joint phase unwrapping and parameters estimation method was proposed in [39] using a recursive processing. This eliminates the need to perform phase unwrapping prior to the estimation process. Rather, the unwrapping is performed sample at a time given the current estimation of the parameters yielding a more robust process.

Let $\hat{\boldsymbol{\eta}}[n] = [\hat{\boldsymbol{\mu}}^T[n], \hat{\boldsymbol{\theta}}^T[n]]^T$, where $\hat{\boldsymbol{\mu}}[n] = [\hat{\mu}_1[n], \dots, \hat{\mu}_M[n]]^T$, be the estimated parameters at the n th step of the filter. Then, the phase is given by

$$\hat{\phi}[n] = \mathbf{H}[n] \hat{\boldsymbol{\eta}}[n] + \varepsilon[n] \quad (61)$$

where

$$\mathbf{H}[n] = \begin{bmatrix} \mathbf{I}_M & \begin{bmatrix} 2\pi n & \pi n^2 \\ \vdots & \vdots \\ 2\pi M n & \pi M n^2 \end{bmatrix} \end{bmatrix} \quad (62)$$

$\hat{\phi}[n] = [\hat{\phi}_1[n], \dots, \hat{\phi}_M[n]]^T$ and $\varepsilon[n] = [\varepsilon_1[n], \dots, \varepsilon_M[n]]^T$. The phase error of the m th harmonic component is defined as $\varepsilon_m = \Im\{e^{-j\mu_m} \text{diag}(\mathbf{s}_m^*) \mathbf{e}_m\}$.

The algorithm is initialized with an estimate given $L \geq M+2$ samples of the unwrapped phase using a conventional unwrapping algorithm, as suggested above,

$$\hat{\boldsymbol{\eta}}[L] = (\mathbf{H}_L^T \mathbf{H}_L)^{-1} \mathbf{H}_L^T \hat{\phi}_L \quad (63)$$

where $\mathbf{H}_L = [\mathbf{H}^T[0], \dots, \mathbf{H}^T[L-1]]^T$ and $\hat{\phi}_L = [\hat{\phi}^T[0], \dots, \hat{\phi}^T[L-1]]^T$. Following the initialization process, the algorithm iterates through three steps for $n = L+1, \dots, N-1$.

- 1) **Predict:** $\hat{\phi}[n+1|n] = \mathbf{H}[n+1] \hat{\boldsymbol{\eta}}[n]$
- 2) **Unwrap:** $\hat{\phi}_m[n+1] = \arg(\hat{s}_m[n+1] e^{-j\hat{\phi}_m[n+1|n]}) + \hat{\phi}_m[n+1|n]$
- 3) **Update:** $\hat{\boldsymbol{\eta}}[n+1] = \hat{\boldsymbol{\eta}}[n] + \mathbf{K}_{n+1} (\hat{\phi}[n+1] - \mathbf{H}[n+1] \hat{\boldsymbol{\eta}}[n])$ where $\mathbf{K}_{n+1} = (\mathbf{H}_{n+1}^T \mathbf{H}_{n+1})^{-1} \mathbf{H}_{n+1}^T$. Note that \mathbf{K}_{n+1} is not data dependent and can be computed off-line.

The estimated parameters are obtained from the final step, $\hat{\boldsymbol{\theta}}^{(\text{SEES})} = \boldsymbol{\theta}[N-1]$. The recursive processing used for the parameters estimation is equivalent to a batch LS estimation given the unwrapped phase [58]. That is,

$$\hat{\boldsymbol{\eta}} \hat{=} \hat{\boldsymbol{\eta}}[N-1] = (\mathbf{H}^T \mathbf{H})^{-1} \mathbf{H}^T \hat{\phi} \quad (64)$$

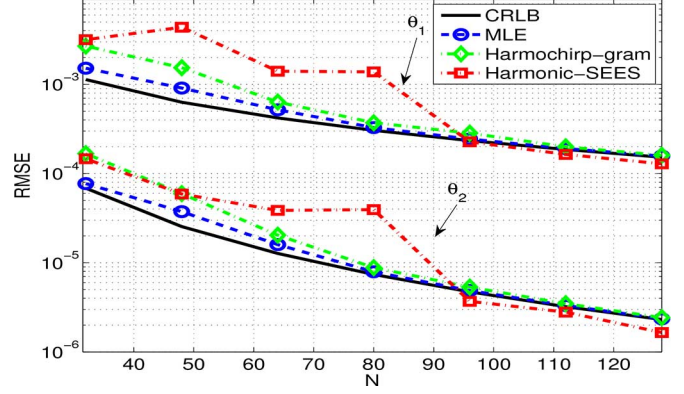


Fig. 5. RMSE for the exact MLE, approximated MLE and Harmonic-SEES including the CRLB vs. the number of samples.

where $\mathbf{H} \triangleq \mathbf{H}_{N-1}$ and $\hat{\phi} \triangleq \hat{\phi}_{N-1}$.

Again, once $\hat{\boldsymbol{\theta}}^{(\text{SEES})}$ is estimated, the number of harmonics can be selected by substituting the estimate into (8) instead of the $\hat{\boldsymbol{\theta}}^{(\text{MLE})}$ for each possible value of M .

C. Accuracy Analysis

We evaluate the bias and covariance of the estimate $\hat{\boldsymbol{\eta}}$ given in (64) when it is estimated in the presence of noise. Since both estimation method are equivalent, the analysis should hold to the estimate in (60). Substituting (58) into (64) yields that the estimate of $\boldsymbol{\eta}$ is given by

$$\hat{\boldsymbol{\eta}} = \boldsymbol{\eta} + (\mathbf{H}^T \mathbf{H})^{-1} \mathbf{H}^T \boldsymbol{\varepsilon} \quad (65)$$

where $\boldsymbol{\varepsilon} = [\varepsilon^T[0], \dots, \varepsilon^T[N-1]]^T$. Note that $E[\varepsilon_m] = E[\Im\{e^{-j\mu_m} \mathbf{s}_m^* \odot \mathbf{e}_m\}] = \Im\{e^{-j\mu_m} \mathbf{s}_m^* \odot \mathbf{G}_m E[\mathbf{v}]\} = \mathbf{0}_N$, where we substitute $\mathbf{G}_m \mathbf{v}$ instead of \mathbf{e}_m . This means that $E[\boldsymbol{\varepsilon}] = \mathbf{0}_{NM}$ and therefore $\hat{\boldsymbol{\eta}}$ is approximately unbiased.

The covariance of $\hat{\boldsymbol{\eta}}$, is given by

$$\begin{aligned} \text{cov}(\hat{\boldsymbol{\eta}}) &= (\mathbf{H}^T \mathbf{H})^{-1} \mathbf{H}^T \text{cov}(\hat{\phi}) \mathbf{H} (\mathbf{H}^T \mathbf{H})^{-1} \\ &= (\mathbf{H}^T \mathbf{H})^{-1} \mathbf{H}^T \text{cov}(\boldsymbol{\varepsilon}) \mathbf{H} (\mathbf{H}^T \mathbf{H})^{-1} \end{aligned} \quad (66)$$

The covariance of the noise, $\text{cov}(\boldsymbol{\varepsilon})$, is a $NM \times NM$ block matrix composed of N^2 blocks of $M \times M$ matrices of the form $\text{cov}(\varepsilon[n] \varepsilon^H[k])$. Using the facts that $E[\Im\{\mathbf{v}\} \Re\{\mathbf{v}\}^T]$ is a zero matrix, while $E[\Re\{\mathbf{v}\} \Re\{\mathbf{v}\}^T] = E[\Im\{\mathbf{v}\} \Im\{\mathbf{v}\}^T] = \sigma_v^2 / 2 \mathbf{I}_N$, it can be shown that

$$E[\varepsilon_m \varepsilon_{m'}] = \frac{\sigma_v^2}{2} \Re\{\text{diag}(\mathbf{s}_m^*) \mathbf{G}_m \mathbf{G}_{m'}^H \text{diag}(\mathbf{s}_{m'}^T)\} \quad (67)$$

Substituting (67) in (66) yields the covariance matrix of $\hat{\boldsymbol{\theta}}$. In the simulation results we show that the asymptotic covariance in (66) coincides with the CRLB. However, this covariance result only holds for large N and small noise.

D. Computational Load

The first step in the Harmonic-SEES method is to create the vector $\bar{\mathbf{x}}_{\ell, m}$ in (42). This is done by multiplying the input with a diagonal matrix \mathbf{D} , which requires $2N$ multiplications, and performing DFT (using FFT), which involves $\mathcal{O}(N \log N)$ multiplications. This is done M times for each possible value. The

TABLE I
COMPARISON OF THE FOUR ESTIMATION METHODS. THRESHOLD SNR AND EFFICIENCY FROM FIG. 6

Method	Complexity	Threshold SNR	Asymptotic Efficiency
MLE	$\mathcal{O}(N^6 M)$	-10dB	Yes
Harmochirp-gram	$\mathcal{O}(N^5 M)$	-10dB	Yes
PHAF	$\mathcal{O}(N^{7/2} L)$	13dB	No
Harmonic-SEES	$\mathcal{O}(N^2 \log N M)$	5dB	Yes

total number of real multiplications required for the de-chirping selection is $\mathcal{O}(N \log N \cdot LM)$. Since the de-chirping process and the DFT block in the frequency filtering part is already performed in the de-chirping selection, no more multiplications are required. Next, the vectors \tilde{s}_m are created in (47) by multiplying each harmonic component with a diagonal matrix \mathbf{Y}_m , which requires $2N$ multiplications. The reconstruction of each harmonic component is $\mathcal{O}(N \log N)$ multiplications, similarly to the de-chirping selection. Therefore, the complexity of the separate step in total is $\mathcal{O}(N \log N \cdot (L + M)M)$. Finally, the estimation of both parameters is done by the recursive process. Since the gain is not data dependent, it can be computed off-line. Therefore each iteration requires $\mathcal{O}(M^2)$ multiplications. since there are N iterations, the total complexity of the estimation process is $\mathcal{O}(NM^2)$. Combining both steps and assuming $L \gg M$ results in a total of $\mathcal{O}(N \log N \cdot LM)$ multiplications. The de-chirping selection is only a rough estimate of θ_2 , therefore there is no need to search with resolution that corresponds to the CRLB and L can be in the order of N . In that case, the total number of real multiplications for the Harmonic-SEES method is therefore $\mathcal{O}(N^2 \log N M)$ which is substantially less than that of the Harmochirp-gram. A comparison between computational complexity of each method is presented in Table I.

The low computational complexity of the proposed algorithm makes it more suitable for real-time applications. Furthermore, due to the recursive implementation of the estimation step, the estimated parameters can be updated on-line.

VIII. NUMERICAL RESULTS

We present numerical examples that compare the performance of the MLE, Harmochirp-gram, PHAF and the proposed Harmonic-SEES methods. We start with synthetic simulations and then present real data results.

A. Simulations

In each simulation we consider $M = 3$ harmonics. The amplitudes of the harmonic components are given as $a_m = 2^{1-m} e^{j\mu_m}$, $m = 1, \dots, M$, where μ_m is a uniformly distributed phase. The noise power σ_v^2 is adjusted to give the desired SNR defined as $\text{SNR} = 10 \log_{10}(\sum_{m=1}^M |a_m|^2 / \sigma_v^2)$ [dB]. In each simulation we evaluated the root mean squared error (RMSE) defined as $\text{RMSE}(\theta_k) = \sqrt{\frac{1}{N_{\text{exp}}} \sum_{i=1}^{N_{\text{exp}}} (\hat{\theta}_{k,i} - \theta_k)^2}$, $k = 1, 2$ where $\hat{\theta}_{1,i}$ and $\hat{\theta}_{2,i}$ are the estimate of θ_1 and θ_2 at the i th trial, respectively and $N_{\text{exp}} = 500$ is the number of Monte-Carlo independent trials. The phases of the amplitudes are generated

once for all trials. For comparison, in each simulation we compared the results with the associated CRLB.

First, we wish to examine the orthogonality assumption, presented in Section IV-B. The parameters of the fundamental chirp are given by $\theta_1 = 0.05$ and $\theta_2 = 10^{-4}$ and the SNR is set to 15 dB. The requirement of the number of samples in (16) in this case is $N \geq 3/\delta = 3/\theta_1 = 60$. The filter's width for the harmonic components separation was 6 samples. We examine the performance of the exact and approximated MLE for number of samples ranging from $N = 16$ up to $N = 128$. The RMSE for both parameters versus the number of samples is presented in Fig. 5. It can be seen that when the number of samples satisfies (16), the Harmochirp-gram performs similarly to the MLE. The Harmonic-SEES method requires more samples and performs well in this case for $N \geq 96$. This is because for smaller number of samples the harmonic components are not well separated and cannot be properly filtered. The peaks of the PHAF becomes wider as the number of samples decreases. For the specified number of samples the peaks were not separable and the PHAF method was unable to detect the three components. Therefore the results are not presented for this case. Next, we compare the RMSE of the estimated normalized initial frequency and frequency rate versus the SNR for the MLE, Harmochirp-gram, PHAF and Harmonic-SEES methods. The parameters of the fundamental chirp are given by $\theta_1 = 0.1$ and $\theta_2 = 10^{-4}$. The number of samples is $N = 512$, far more than the requirement in (16). For the PHAF method, $L = 4$ lags are used with $\tau = [50, 100, 150, 200]$ samples. We consider SNR values from -15 [dB] to 21 [dB] in steps of 2 [dB]. Those settings are used in the simulations hereafter unless otherwise stated. The RMSE results are presented in Fig. 6. The CRLB and the theoretical lower bound of the PHAF method, according to (38), are also plotted for both parameters. The MLE and Harmochirp-gram perform similarly and achieve the CRLB for both parameters. For SNR above 5 [dB] the Harmonic-SEES method also achieves the CRLB. The PHAF estimator does not reach its lower bound. This is expected as it is not a tight bound. The error seems to converge to around 1.5 times the lower bound for SNR of 13 [dB] or more.

Fig. 7 present the scattering of the estimate errors, i.e., $\varepsilon_1 = \hat{\theta}_1 - \theta_1$, $\varepsilon_2 = \hat{\theta}_2 - \theta_2$, of the MLE and Harmonic-SEES methods along with a theoretical and actual 50% confidence level ellipses for SNR values of -1 [dB] and 7 [dB]. For the lower SNR value, the Harmonic-SEES method does not achieve the CRLB and thus the actual confidence level ellipse is larger than the theoretical one. For the higher SNR the ellipse of the Harmonic-SEES coincides with that of the CRLB.

We now compare the performance of the model order selection using the MDL and AIC criteria for the MLE, PHAF and Harmonic-SEES methods. We evaluate the probability of detecting the correct model order, p_d defined as $p_d = \frac{1}{N_{\text{exp}}} \sum_{i=1}^{N_{\text{exp}}} \mathbb{1}_{M=M}$ where $\mathbb{1}$ is the indicator function. The p_d versus SNR results are presented in Fig. 8. For both MDL and AIC criteria, the model order estimator that uses the Harmonic-SEES always estimates correctly for SNR values of 5 [dB] or more. Not surprisingly, this is the threshold SNR for which the CRLB is achieved. The AIC performs slightly better than the MLE for both MLE and the Harmonic-SEES

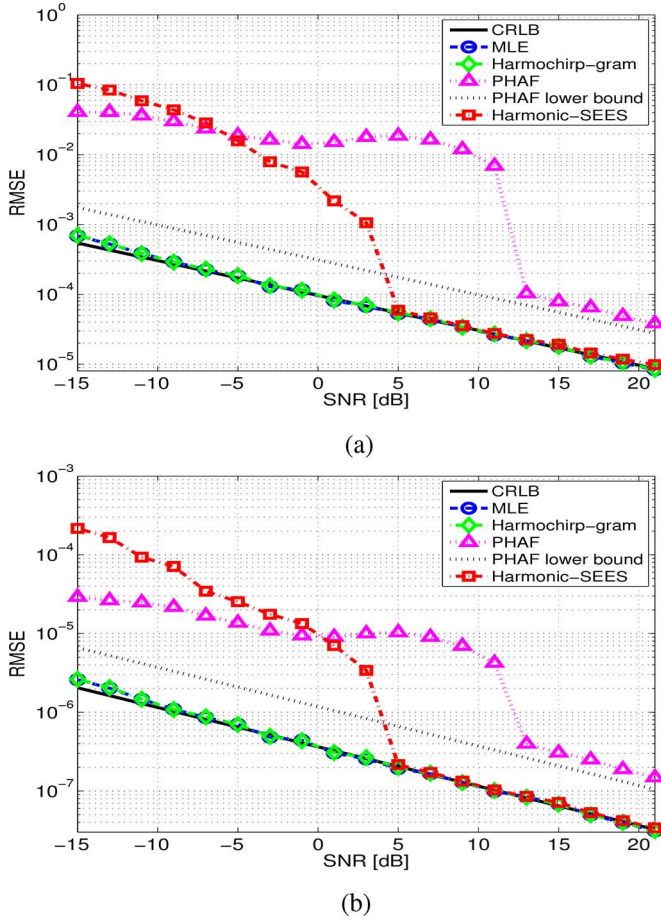


Fig. 6. RMSE for each estimator including the CRLB vs. SNR. (a) θ_1 , Normalized initial frequency, (b) θ_2 , Normalized frequency rate.

estimator. The PHAF method achieves perfect selection at around 11 [dB] with both criteria perform equally.

Finally, we evaluate the sensitivity of the Harmonic-SEES method and the MLE to vibrations in the frequency. The m th harmonic component is simulated with an instantaneous frequency given by $f_m[n] = m(\theta_1(1 + \delta_f \cdot \sin(2\pi f_v n)) + \theta_2 n)$. The SNR is fixed to 10 [dB] and we examine different values of both parameters, δ_f and f_v . The RMSE versus δ_f is presented in Fig. 9 for both estimated parameters, where each plot shows the error for different values of f_v . The PHAF performed poorly in this case and the results are not presented. Clearly, the estimator is very sensitive to changes in the assumed frequency model. The performance of the estimator is better for higher values of f_v . For the highest value of f_v , the proposed method performs similarly to the MLE for $\delta_f \leq 0.3$, which is 30% from the initial frequency.

B. Real Data

We demonstrate the model order selection and the parameter estimation of a recording of an echolocation call produced by an *E. nilssonii* bat [59]. The signal is sampled at 125 kHz and divided into segments of $N = 300$ samples. In each segment, the parameter and model order were estimated using the AIC criterion. A spectrogram of the signal is presented in Fig. 10. The signal seems to have four harmonic components but the last one

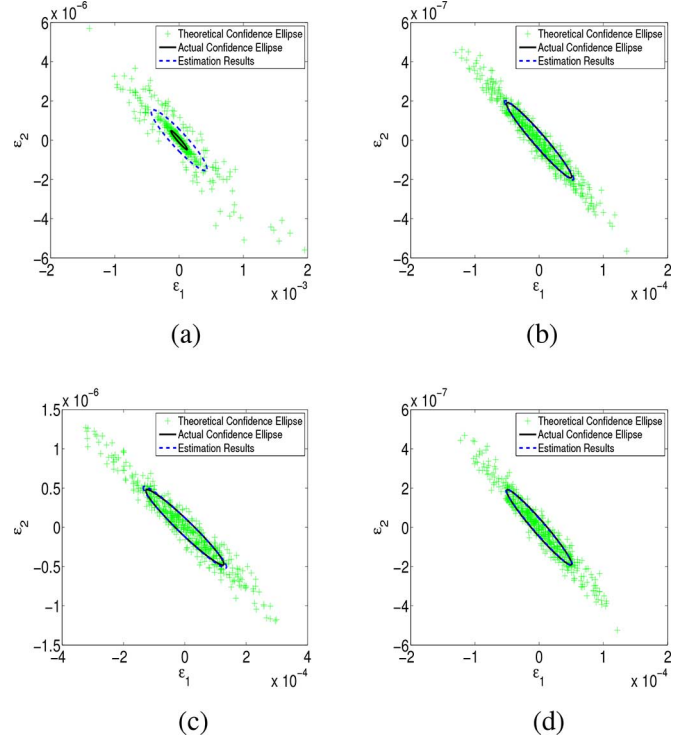


Fig. 7. The estimates and confidence ellipses of the fundamental frequency and frequency rate for (a) Harmonic-SEES, SNR = 7 [dB], (b) Harmonic-SEES, SNR = -1 [dB], (c) MLE, SNR = 7 [dB], (d) MLE, SNR = -1 [dB].

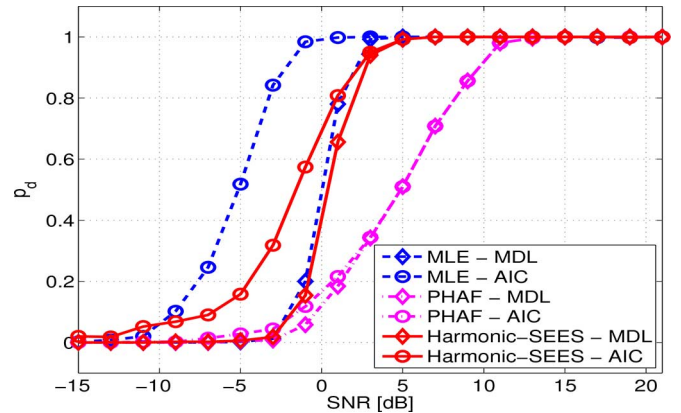


Fig. 8. Probability of correct model order selection for each estimator.

is very weak and is hardly detected. The estimated frequencies are plotted in dashes line on top of the spectrogram and the selected model order, using the AIC criterion, is plotted above. The results for the MDL were very similar and thus not presented. The markers on the spectrogram corresponds to a peak detection at each time frame. Clearly, the fundamental chirp is less dominant, yet it is detected the entire time.

Next, we demonstrate the model order selection and the parameter estimation of a recording of an echolocation call produced by a *G. melas* whale [60]. The signal is sampled to 44.1 kHz. Again, the signal is divided into segments of $N = 300$ samples and the results are presented in Fig. 11 in the same format as the previous example. Once again, the AIC and MDL performed similarly and the latter is not presented. The fundamental frequency line is always detected. The higher harmonics,

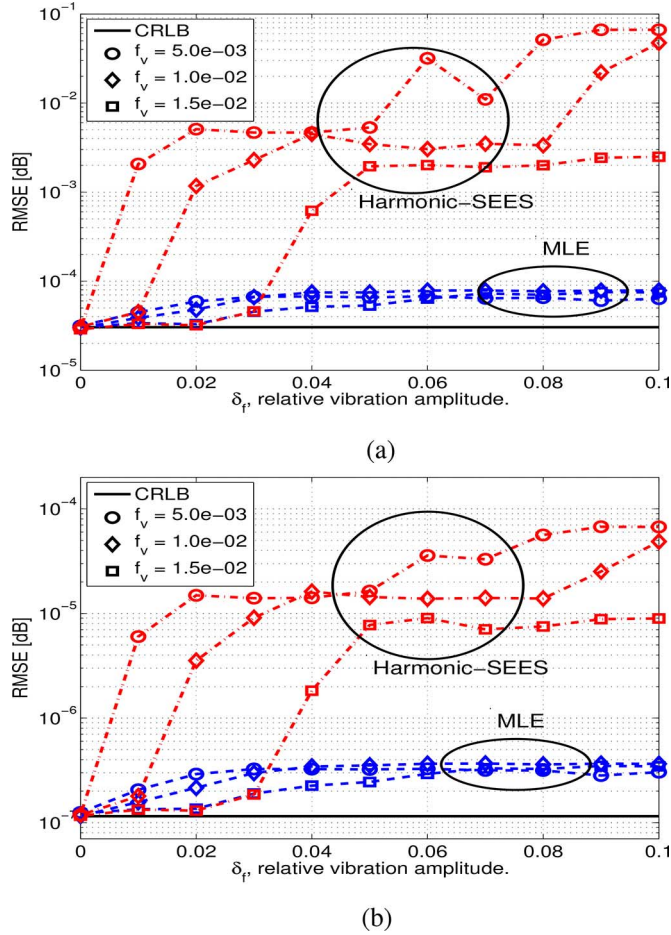


Fig. 9. RMSE of the Harmonic-SEES estimator and the MLE versus vibrations in the instantaneous frequency. (a) θ_1 , Normalized initial frequency, (b) θ_2 , Normalized frequency rate.

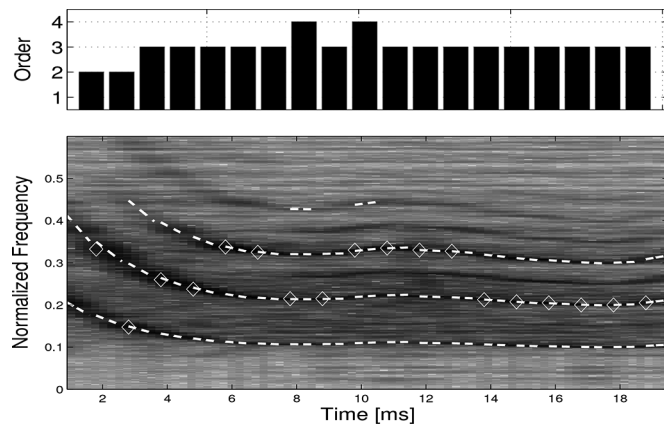


Fig. 10. Model order selection and parameter estimation of an echolocation call produced by an *E. Nilssonii* bat. The diamonds mark peaks detection in the spectrogram.

starting from the 5th, are very weak and not detected most of the time. The first part of the signal contains an interference which is not detected. The interference is relatively strong, comparing to each harmonic component, but not strong enough when combining all the harmonic components together.

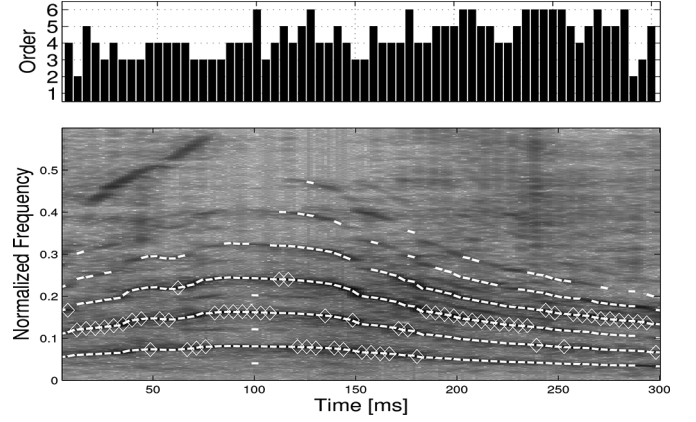


Fig. 11. Model order selection and parameter estimation of an echolocation call produced by a *G. melas* whale. The diamonds mark peaks detection in the spectrogram.

IX. CONCLUSION

We have considered the problem of estimating the fundamental initial frequency and frequency rate of harmonic linear chirps when the number of harmonic components is unknown. In order to estimate the number of harmonics, we presented a model order selection criteria based on maximum likelihood. The exact and approximated MLE have large computation load due to a two-dimensional exhaustive search in the parameter space. We suggested a two-step estimation method that first separates the signal to its harmonic components, and then estimates the two parameters of interest using a joint least squares method given the phases of the harmonic components. The computational complexity of the proposed estimator is much smaller than that of the maximum likelihood estimators. We also presented the PHAF method and compared it to the proposed method. Simulations show that the proposed two-step estimator achieves the CRLB at moderate or high signal to noise ratio and that the suboptimal estimators can be used instead of the MLE in order to estimate the number of harmonics. Real data examples demonstrate the performance of the proposed method on echolocation calls.

APPENDIX

In this Appendix we present a detailed derivation of the submatrices of the FIM in (17) following [54]. The (1, 1)th element of $J_{\theta, \theta}$ is the FIM $J_{\theta_1, \theta_1} = \frac{2}{\sigma_v^2} \Re \{ \mathbf{a}^H \frac{\partial \mathbf{S}^H}{\partial \theta_1} \frac{\partial \mathbf{S}}{\partial \theta_1} \mathbf{a} \}$ where $\frac{\partial \mathbf{S}}{\partial \theta_1} = [\frac{\partial s_1}{\partial \theta_1}, \dots, \frac{\partial s_M}{\partial \theta_1}]$. By substituting s_m we get that $\frac{\partial s_m}{\partial \theta_1} = j2\pi m \mathbf{q} \odot s_m$, where $\mathbf{q} = [0, 1, \dots, N-1]^T$. Substituting $\frac{\partial s_m}{\partial \theta_1}$ in $\frac{\partial \mathbf{S}}{\partial \theta_1}$ results in $\frac{\partial \mathbf{S}}{\partial \theta_1} = j2\pi \mathbf{q} \mathbf{p}^T \odot \mathbf{S}$, where $\mathbf{p} = [1, 2, \dots, M]^T$ and \odot is the Hadamard (dot) product. Using $\frac{\partial \mathbf{S}}{\partial \theta_1}$ yields,

$$J_{\theta_1, \theta_1} = \frac{2}{\sigma_v^2} (2\pi)^2 \| (\mathbf{q} \mathbf{p}^T \odot \mathbf{S}) \mathbf{a} \|^2 = \frac{8\pi^2}{\sigma_v^2} \| \mathbf{QSDa} \|^2 \quad (68)$$

where in the second transition we used the result $(\mathbf{q} \mathbf{p}^T \odot \mathbf{S}) \mathbf{a} = \mathbf{q} \odot (\mathbf{SDa}) = \mathbf{QSDa}$, and in the second transition we used the identity $\mathbf{a} \odot \mathbf{b} = \text{diag}(\mathbf{a}) \odot \mathbf{b}$ for two vectors with identical dimensions, \mathbf{a} and \mathbf{b} .

The (2, 2)th element of $\mathbf{J}_{\boldsymbol{\theta},\boldsymbol{\theta}}$ is the FIM $J_{\theta_2,\theta_2} = \frac{2}{\sigma_v^2} \Re\{\mathbf{a}^H \frac{\partial \mathbf{S}^H}{\partial \theta_2} \frac{\partial \mathbf{S}}{\partial \theta_2} \mathbf{a}\}$ where $\frac{\partial \mathbf{S}}{\partial \theta_2} = [\partial \mathbf{s}_1/\partial \theta_2, \dots, \partial \mathbf{s}_M/\partial \theta_2]$. By substituting \mathbf{s}_m we get that $\partial \mathbf{s}_m/\partial \theta_2 = j\pi m \mathbf{u} \odot \mathbf{s}_m$, where $\mathbf{u} = [0, 1^2, \dots, (N-1)^2]^T$. Substituting $\partial \mathbf{s}_m/\partial \theta_2$ in $\partial \mathbf{S}/\partial \theta_2$ yields $\partial \mathbf{S}/\partial \theta_2 = j\pi \mathbf{u} \mathbf{p}^T \odot \mathbf{S}$. Using $\partial \mathbf{S}/\partial \theta_2$ yields,

$$J_{\theta_2,\theta_2} = \frac{2}{\sigma_v^2} (\pi)^2 \|(\mathbf{u} \mathbf{p}^T \odot \mathbf{S}) \mathbf{a}\|^2 = \frac{2\pi^2}{\sigma_v^2} \|\mathbf{Q}^2 \mathbf{S} \mathbf{D} \mathbf{a}\|^2 \quad (69)$$

where in the second transition we used a similar result to the identity expressed in (68) where the vector \mathbf{q} is replaced by the vector \mathbf{u} .

The (1, 2)th element of $\mathbf{J}_{\boldsymbol{\theta},\boldsymbol{\theta}}$ is the FIM $J_{\theta_1,\theta_2} = \frac{2}{\sigma_v^2} \Re\{\mathbf{a}^H \frac{\partial \mathbf{S}^H}{\partial \theta_1} \frac{\partial \mathbf{S}}{\partial \theta_2} \mathbf{a}\}$. Using $\partial \mathbf{S}/\partial \theta_1$ and $\partial \mathbf{S}/\partial \theta_2$ yields,

$$\begin{aligned} J_{\theta_1,\theta_2} &= \frac{2}{\sigma_v^2} (2\pi)(\pi) \Re\{\mathbf{a}^H (\mathbf{q} \mathbf{p}^T \odot \mathbf{S})^H (\mathbf{u} \mathbf{p}^T \odot \mathbf{S}) \mathbf{a}\} \\ &= \frac{4\pi^2}{\sigma_v^2} \|\mathbf{Q}^{3/2} \mathbf{S} \mathbf{D} \mathbf{a}\|^2 \end{aligned} \quad (70)$$

We next derive the sub-matrices of the FIM $\mathbf{J}_{\mathbf{a},\mathbf{a}}$. We use the identity $\Re\{jx\} = -\Im\{x\}$ for a complex scalar x .

The upper-left sub-matrix of $\mathbf{J}_{\mathbf{a},\mathbf{a}}$ is $\mathbf{J}_{\mathbf{a}_r,\mathbf{a}_r} = \frac{2}{\sigma_v^2} \Re\{\frac{\partial (\mathbf{S} \mathbf{a})^H}{\partial \mathbf{a}_r} \frac{\partial \mathbf{S} \mathbf{a}}{\partial \mathbf{a}_r}\} = \frac{2}{\sigma_v^2} \Re\{\mathbf{S}^H \mathbf{S}\}$. Similarly, we define the other sub-matrices of $\mathbf{J}_{\mathbf{a},\mathbf{a}}$. The upper-left sub-matrix of $\mathbf{J}_{\boldsymbol{\theta},\mathbf{a}}$ is $\mathbf{J}_{\theta_1,\mathbf{a}_r} = \frac{2}{\sigma_v^2} \Re\{\frac{\partial (\mathbf{S} \mathbf{a})^H}{\partial \theta_1} \frac{\partial \mathbf{S} \mathbf{a}}{\partial \mathbf{a}_r}\} = \frac{4\pi}{\sigma_v^2} \Im\{\mathbf{a}^H \mathbf{D}^T \mathbf{S}^H \mathbf{Q} \mathbf{S}\}$ where we used the expression of $\partial \mathbf{S}/\partial \theta_1$. Similarly, the upper-right sub-matrix of the FIM $\mathbf{J}_{\boldsymbol{\theta},\mathbf{a}}$ is $\mathbf{J}_{\theta_2,\mathbf{a}_r}$. In a similar way we derive $\mathbf{J}_{\theta_1,\mathbf{a}_i}$. The lower-left sub-matrix of the FIM $\mathbf{J}_{\boldsymbol{\theta},\mathbf{a}}$ is $\mathbf{J}_{\theta_2,\mathbf{a}_r} = \frac{2}{\sigma_v^2} \Re\{\frac{\partial (\mathbf{S} \mathbf{a})^H}{\partial \theta_2} \frac{\partial \mathbf{S} \mathbf{a}}{\partial \mathbf{a}_r}\} = \frac{2\pi}{\sigma_v^2} \Im\{\mathbf{a}^H \mathbf{D}^T \mathbf{S}^H \mathbf{Q}^2 \mathbf{S}\}$ where we used again $\partial \mathbf{S}/\partial \theta_2$. In a similar way we derive $\mathbf{J}_{\theta_2,\mathbf{a}_i}$. This concludes the derivation of the FIM.

ACKNOWLEDGMENT

The authors would like to thank the associate editor and the anonymous reviewers for their insightful and constructive comments which helped to improve and clarify the paper.

REFERENCES

- [1] M. G. Christensen, P. Stoica, A. Jakobsson, and H. S. Jensen, "Multi-pitch estimation," *Signal Process.*, vol. 88, no. 4, pp. 972–983, Apr. 2008.
- [2] M. G. Christensen, S. H. Jensen, A. Jakobsson, and S. H. Jensen, "Optimal filter designs for fundamental frequency estimation," *IEEE Signal Process. Lett.*, vol. 15, no. 7, pp. 745–748, Dec. 2008.
- [3] C. Dubois and M. Davy, "Joint detection and tracking of time varying harmonic components: A flexible Bayesian approach," *IEEE Trans. Audio, Speech, Lang. Process.*, vol. 15, no. 4, pp. 1283–1295, May 2007.
- [4] H. Li, P. Stoica, and J. Li, "Computationally efficient parameter estimation for harmonic sinusoidal signals," *Signal Process.*, vol. 80, no. 9, pp. 1937–1944, Sep. 2000.
- [5] K. W. Chan and H. C. So, "Accurate frequency estimation for real harmonic sinusoids," *IEEE Signal Process. Lett.*, vol. 11, no. 7, pp. 609–612, Jul. 2004.
- [6] A. Nehorai and B. Porat, "Adaptive comb filtering for harmonic signal enhancement," *IEEE Trans. Acoust., Speech, Signal Process.*, vol. 34, no. 5, pp. 1124–1138, Oct. 1986.
- [7] M. Hinich, "Detecting a hidden periodic signal when its period is unknown," *IEEE Trans. Acoust., Speech, Signal Process.*, vol. 30, no. 5, pp. 747–750, Oct. 1982.
- [8] T. W. Eddy, "Maximum likelihood detection and estimation for harmonic sets," *J. Acoust. Soc. Amer.*, vol. 68, no. 1, pp. 149–155, Jul. 1980.

- [9] A. Swami and M. Ghogho, "Cramer-Rao bounds for coupled harmonics in noise," in *Proc. 31st Asilomar Conf. Signals, Syst. Comput.*, Pacific Grove, CA, USA, Nov. 1997, vol. 1, pp. 483–487.
- [10] G. W. Chang and C. Chen, "An accurate time domain procedure for harmonics and inter-harmonics detection," *IEEE Trans. Power Del.*, vol. 25, no. 3, pp. 1787–1795, Jul. 2010.
- [11] S. K. Jain and S. N. Singh, "Exact model order ESPRIT technique for harmonics and inter-harmonics estimation," *IEEE Trans. Instrum. Meas.*, vol. 61, no. 7, pp. 1915–1923, Jul. 2012.
- [12] E. Chassande-Moffin and P. Flandrin, "On the time frequency detection of chirps," *Appl. Computat. Harmon. Analysis*, vol. 6, no. 2, pp. 252–181, Mar. 1999.
- [13] M. Vespe, G. Jones, and C. Baker, "Lessons for radar: Waveform diversity in echolocating mammals," *IEEE Signal Process. Mag.*, vol. 26, no. 1, pp. 65–75, Jan. 2009.
- [14] Y. Kopsinis, E. Aboutanios, D. A. Waters, and S. McLaughlin, "Time-frequency and advanced frequency estimation techniques for the investigation of bat echolocation calls," *J. Acoust. Soc. Amer.*, vol. 127, no. 2, pp. 1124–1134, 2010.
- [15] M. Bennett, S. McLaughlin, T. Anderson, and N. McDicken, "Filtering of chirped ultrasound echo signals with the fractional Fourier transform," in *Proc. IEEE Ultrason. Symp.*, Aug. 2004, vol. 3, pp. 2036–2040.
- [16] T. H. Chung and J. Cheung, "Maximum likelihood estimation of direction of arrival and frequency sweeping rate with linear chirp signals," *IEEE Signal Process. Lett.*, vol. 2, no. 8, pp. 163–165, Aug. 1995.
- [17] R. Aouada, A. Belouchrani, and K. Abed-Meraim, "Multipath parameter estimation of linear chirp signals using sensor arrays," in *Proc. IEEE-SAM*, July 2004, pp. 313–317.
- [18] S. Peleg and B. Porat, "Estimation and classification of polynomial-phase signals," *IEEE Trans. Inf. Theory*, vol. 37, no. 2, pp. 422–430, Mar. 1991.
- [19] S. Peleg and B. Friedlander, "The discrete polynomial-phase transform," *IEEE Trans. Signal Process.*, vol. 43, no. 8, pp. 1901–1914, Aug. 1995.
- [20] A. Amar, A. Leshem, and A. J. van-der Veen, "A computationally efficient blind estimator of polynomial phase signals observed by a sensor array," *IEEE Trans. Signal Process.*, vol. 58, no. 9, pp. 4674–4683, Sep. 2010.
- [21] R. P. Perry, R. C. DiPietro, and R. Fante, "SAR imaging of moving targets," *IEEE Trans. Aerosp. Electron. Syst.*, vol. 35, no. 1, pp. 188–200, Jan. 1999.
- [22] N. Rankine, M. Stevenson, M. Mesbah, and B. Boashash, "A nonstationary model of newborn EEG," *IEEE Trans. Biomed. Eng.*, vol. 54, no. 1, pp. 19–28, Jan. 2007.
- [23] S. Barbarossa, A. Scaglione, and G. Giannakis, "Product high-order ambiguity function for multicomponent polynomial-phase signal modeling," *IEEE Trans. Signal Process.*, vol. 46, no. 3, pp. 691–708, Mar. 1998.
- [24] G. T. Whipps and R. L. Moses, "A combined order selection and parameter estimation algorithm for coupled harmonics," in *Proc. Military Sensing Symp. (MSS) Specialty Group on Battlefield Acoust. Seismic Sens., Magn. Electr. Field Sens.*, Laurel, MD, USA, 2003.
- [25] T. J. Abatzoglou, "Fast maximum likelihood joint estimation of frequency and frequency rate," *IEEE Trans. Aerosp. Electron. Syst.*, vol. 22, no. 6, pp. 708–715, Nov. 1986.
- [26] R. Kumaresan and S. Verma, "On estimating the parameters of chirp signals using rank reduction techniques," in *Proc. 21st Asilomar Conf. Signals, Syst. Comput.*, Pacific Grove, CA, USA, 1987, pp. 555–558.
- [27] B. Volcker and B. Ottersten, "Chirp parameter estimation using rank reduction," in *Proc. 32nd Asilomar Conf. Signals, Syst. Comput.*, Pacific Grove, CA, USA, Nov. 1998, vol. 2, pp. 1443–1446.
- [28] S. Peleg and B. Porat, "Linear FM signal parameter estimation from discrete-time observations," *IEEE Trans. Aerosp. Electron. Syst.*, vol. 27, no. 4, pp. 607–616, Jul. 1991.
- [29] P. O'Shea, "Fast parameter estimation algorithms for linear FM signals," in *Proc. IEEE Int. Conf. Acoust., Speech, Signal Process. (ICASSP)*, Adelaide, Australia, Apr. 1994, vol. 4, pp. 17–20.
- [30] S. Barbarossa, "Analysis of multicomponent LFM signals by a combined Wigner-Hough transform," *IEEE Trans. Signal Process.*, vol. 43, no. 6, pp. 1511–1515, Jun. 1995.
- [31] S. Saha and S. M. Kay, "Maximum likelihood parameter estimation of superimposed chirps using Monte Carlo importance sampling," *IEEE Trans. Signal Process.*, vol. 50, no. 2, pp. 224–230, Feb. 2002.
- [32] C. Lin and P. M. Djuric, "Estimation of chirp signals by MCMC," in *Proc. IEEE Int. Conf. Acoust., Speech, Signal Process. (ICASSP)*, Istanbul, Turkey, Jun. 2000, vol. 1, pp. 265–268.
- [33] L. Qi, R. Tao, S. Zhou, and Y. Wang, "Detection and parameter estimation of multicomponent LFM signal based on the fractional Fourier transform," *Sci. China Series F: Inf. Sci.*, vol. 47, no. 2, pp. 184–198, 2004.

- [34] P. Wang, H. Li, and B. Himed, "Parameter estimation of linear frequency-modulated signals using integrated cubic phase function," in *Proc. 42nd Asilomar Conf. Signals, Syst. Comput.*, Pacific Grove, CA, USA, Oct. 2008, pp. 487–491.
- [35] B. Porat, *Digital Processing of Random Signals: Theory and Methods*. Englewood Cliffs, NJ, USA: Prentice-Hall, 1994.
- [36] S. Peleg and B. Friedlander, "A technique for estimating the parameters of multiple polynomial phase signals," in *Proc. Symp. Time-Freq. Time-Scale Anal.*, Victoria, BC, Oct. 1992, pp. 119–122.
- [37] S. Peleg and B. Friedlander, "Multicomponent signal analysis using the polynomial-phase transform," *IEEE Trans. Aerosp. Electron. Syst.*, vol. 32, no. 1, pp. 378–387, Jan. 1996.
- [38] P. M. Djuric and S. M. Kay, "Parameter estimation of chirp signals," *IEEE Trans. Acoust., Speech, Signal Process.*, vol. 38, no. 12, pp. 2118–2126, Dec. 1990.
- [39] B. J. Slocumb and J. Kitchen, "A polynomial phase parameter estimation-phase unwrapping algorithm," in *Proc. IEEE Int. Conf. Acoust., Speech, Signal Process. (ICASSP)*, Adelaide, Australia, Apr. 1994, vol. 4, pp. 129–132.
- [40] S. Barbarossa, "Detection and estimation of the instantaneous frequency of polynomial-phase signals by multilinear time-frequency representations," in *Proc. IEEE Signal Process. Workshop Higher Order Stat.*, Lake Tahoe, CA, Jun. 1993, pp. 168–172.
- [41] M. Z. Ikram, K. Abed-Meraim, and Y. Hua, "Estimating the parameters of chirp signals: An iterative approach," *IEEE Trans. Signal Process.*, vol. 46, no. 12, pp. 3436–3441, Dec. 1998.
- [42] B. Barkat and B. Boashash, "Instantaneous frequency estimation of polynomial FM signals using the peak of the PWVD: Statistical performance in the presence of additive Gaussian noise," *IEEE Trans. Signal Process.*, vol. 47, no. 9, pp. 2480–2490, Sep. 1999.
- [43] J. Angeby, "Estimating signal parameters using the nonlinear instantaneous least squares approach," *IEEE Trans. Signal Process.*, vol. 48, no. 10, pp. 2721–2732, Oct. 2000.
- [44] M. Farquharson, P. O'Shea, and G. Ledwich, "A computationally efficient technique for estimating the parameters of polynomial-phase signals from noisy observations," *IEEE Trans. Signal Process.*, vol. 53, no. 8, pp. 3337–3342, Aug. 2005.
- [45] P. Wang, I. Djurovic, and J. Yang, "Generalized high-order phase function for parameter estimation of polynomial phase signal," *IEEE Trans. Signal Process.*, vol. 56, no. 7, pp. 3023–3028, Jul. 2008.
- [46] P. Wang, H. Li, I. Djurovic, and B. Himed, "Instantaneous frequency rate estimation for high-order polynomial-phase signals," *IEEE Signal Process. Lett.*, vol. 16, no. 9, pp. 782–785, Sep. 2009.
- [47] Y. Wu, H. C. So, and H. Liu, "Subspace-based algorithm for parameter estimation of polynomial phase signals," *IEEE Trans. Signal Process.*, vol. 56, no. 10, pp. 4977–4983, Oct. 2008.
- [48] D. S. Pham and A. M. Zoubir, "Analysis of multicomponent polynomial phase signals," *IEEE Trans. Signal Process.*, vol. 55, no. 1, pp. 56–65, Jan. 2007.
- [49] P. O'Shea, "Improving polynomial phase parameter estimation by using nonuniformly spaced signal sample methods," *IEEE Trans. Signal Process.*, vol. 60, no. 7, pp. 3405–3414, Jul. 2012.
- [50] P. Stoica and Y. Selen, "Model order selection: A review of information criterion rules," *IEEE Signal Process. Mag.*, vol. 21, no. 4, pp. 36–47, Jul. 2004.
- [51] P. M. Djuric, "A model selection rule for sinusoids in white Gaussian noise," *IEEE Trans. Signal Process.*, vol. 44, no. 7, pp. 1744–1751, Jul. 1996.
- [52] M. G. Christensen, A. Jakobsson, and S. H. Jensen, "Sinusoidal order estimation using angles between subspaces," *EURASIP J. Adv. Signal Process.*, vol. 2009, pp. 1–11, Jan. 2009.
- [53] M. G. Christensen, L. J. Højvang, A. Jakobsson, and S. H. Jensen, "Joint fundamental frequency and order estimation using optimal filtering," *EURASIP J. Adv. Signal Process.*, vol. 2011, no. 1, pp. 1–18, Jun. 2011.
- [54] H. Van Trees, *Detection, Estimation, and Modulation Theory—Part IV, Optimum Array Processing*. New York, NY, USA: Wiley, 2004.
- [55] X. G. Xia, "Discrete chirp-Fourier transform and its application to chirp rate estimation," *IEEE Trans. Signal Process.*, vol. 48, no. 11, pp. 3122–3133, Nov. 2000.
- [56] F. J. Harris, "On the use of windows for harmonic analysis with the discrete Fourier transform," *Proc. IEEE*, vol. 66, no. 1, pp. 51–83, Jan. 1978.
- [57] N. Hurley and R. Scott, "Comparing measures of sparsity," *IEEE Trans. Inf. Theory*, vol. 55, no. 10, pp. 4723–4741, Oct. 2009.
- [58] J. M. Mendel, *Lessons in Digital Estimation Theory*. Englewood Cliffs, NJ, USA: Prentice-Hall, 1986.
- [59] G. Pflazer, Avisoft Bioacoustics, European Bat Calls [Online]. Available: <http://www.batcalls.com>
- [60] Interdisciplinary Center for Bioacoustics and Environmental Research [Online]. Available: <http://www.unipv.it/cibra/>



Yaron Doweck (S'14) received the B.Sc. degree (*cum laude*) in electrical engineering in 2012 from the Technion—Israel Institute of Technology.

In 2010, he joined the Signal Processing Department at Rafael, Haifa. He is currently pursuing the M.Sc. degree in electrical engineering at the Technion. His research interests are statistical signal processing and array processing.

Alon Amar (S'04–M'09) received the B.Sc. degree (*cum laude*) in electrical engineering from the Technion—Israel Institute of Technology, in 1997, and the M.Sc. and Ph.D. degrees in electrical engineering from Tel Aviv University, Tel Aviv, Israel, in 2003, and 2009, respectively.

Between 2009 and 2010, he was a Postdoctoral Research Associate with the Circuits and Systems group, Faculty of Electrical Engineering, Mathematics and Computer Science, Delft University of Technology, Delft, The Netherlands. In 2011, he joined Rafael as a Research Scientist at the Signal Processing Department. His main research interests include array signal processing, wireless communication, and sensor networks.



Israel Cohen (M'01–SM'03–F'15) received the B.Sc. (*summa cum laude*), M.Sc., and Ph.D. degrees in electrical engineering from the Technion—Israel Institute of Technology, Haifa, Israel, in 1990, 1993, and 1998, respectively.

He is a Professor of electrical engineering at the Technion—Israel Institute of Technology. From 1990 to 1998, he was a Research Scientist with RAFAEL Research Laboratories, Haifa, Ministry of Defense. From 1998 to 2001, he was a Postdoctoral Research Associate with the Computer Science Department, Yale University, New Haven, CT, USA. In 2001, he joined the Electrical Engineering Department, Technion. His research interests are statistical signal processing, analysis and modeling of acoustic signals, speech enhancement, noise estimation, microphone arrays, source localization, blind source separation, system identification, and adaptive filtering. He is a coeditor of the Multichannel Speech Processing Section of the *Springer Handbook of Speech Processing* (New York: Springer, 2008), a coauthor of *Noise Reduction in Speech Processing* (New York: Springer, 2009), and a coeditor of *Speech Processing in Modern Communication: Challenges and Perspectives* (New York: Springer, 2010).

Dr. Cohen is a General Co-Chair of the 2010 International Workshop on Acoustic Echo and Noise Control (IWAENC). He served as Guest Editor of the *European Association for Signal Processing Journal on Advances in Signal Processing* Special Issue on Advances in Multimicrophone Speech Processing and the *Elsevier Speech Communication Journal* a Special Issue on Speech Enhancement.

Dr. Cohen was a recipient of the Alexander Goldberg Prize for Excellence in Research, and the Muriel and David Jacknow Award for Excellence in Teaching. He serves as a member of the IEEE Audio and Acoustic Signal Processing Technical Committee and the IEEE Speech and Language Processing Technical Committee. He served as Associate Editor of the IEEE TRANSACTIONS ON AUDIO, SPEECH, AND LANGUAGE PROCESSING and the IEEE SIGNAL PROCESSING LETTERS.